

## Google Earth as a data source for investigating river forms and processes: Discriminating river types using form-based process indicators

|                               |  |
|-------------------------------|--|
| Journal:                      | <i>Earth Surface Processes and Landforms</i>   |
| Manuscript ID                 | ESP-19-0096.R1   |
| Wiley - Manuscript type:      | Research Article   |
| Date Submitted by the Author: | n/a  |
| Complete List of Authors:     | Henshaw, Alexander; Queen Mary University of London, School of Geography<br>Sekarsari, Prima; Queen Mary University of London, School of Geography; University of Trento, Civil, Environmental and Mechanical Engineering<br>Guido, Zolezzi; Università di Trento, Dipartimento di Ingegneria Civile, Ambientale e Meccanica<br>Gurnell, Angela; Queen Mary, University of London, Geography |
| Keywords:                     | Google Earth, geomorphic units, river classification, form, process  |
|                               |  |

SCHOLARONE™  
Manuscripts

1  
2  
3 1 **Google Earth as a data source for investigating river forms and processes:**  
4  
5 2 **Discriminating river types using form-based process indicators**  
6  
7  
8 3  
9

10 4 Alexander J. Henshaw<sup>1\*</sup>, Prima W. Sekarsari<sup>1,2</sup>, Guido Zolezzi<sup>2</sup> and Angela M. Gurnell<sup>1</sup>

11  
12 5 <sup>1</sup> School of Geography, Queen Mary University of London, London, UK

13  
14 6 <sup>2</sup> Department of Civil, Environmental and Mechanical Engineering, University of  
15  
16  
17 7 Trento, Trento, Italy

18  
19 8 \* Corresponding author: Alex Henshaw, School of Geography, Queen Mary University  
20  
21 9 of London, Mile End Road, London, E1 4NS, UK; a.henshaw@qmul.ac.uk; +44 (0)207  
22  
23  
24 10 882 5436  
25

26  
27  
28 12 **ABSTRACT**  
29

30  
31 13 Google Earth provides potential for exploiting an enormous reservoir of freely-  
32  
33 14 available remotely sensed data to support river science and management. In this  
34  
35 15 paper, we consider how the platform can support investigation of river physical forms  
36  
37 16 and processes by developing an empirically-based reach-scale classification of semi-  
38  
39 17 natural European single thread to transitional rivers. Using strict reach and image  
40  
41 18 selection criteria, we identified 194 reaches of 68 rivers for analysis. Measurements of  
42  
43 19 channel dimensions and counts of in-channel and floodplain features, standardised  
44  
45 20 for reach length and channel width where necessary, were used to derive a series of  
46  
47 21 geomorphologically-relevant process indicators. A suite of multivariate analyses were  
48  
49 22 then applied to this data set, resulting in the discrimination of five river types: laterally  
50  
51 23 stable, laterally active sinuous-meandering; transitional (near-braided); bedrock; and  
52  
53 24 cascade/step dominated. The results of the classification were tested by examining  
54  
55 25 the characteristics and distribution of the river classes in relation to known independent  
56  
57  
58  
59  
60

1  
2  
3 1 controls of river form including reach-scale energy and valley confinement conditions.  
4  
5 2 Our results show that if methods of data extraction are carefully developed, physically  
6  
7 3 meaningful river reach discrimination can be achieved using Google Earth. Although  
8  
9  
10 4 there are limits to the types of information that can be extracted such that field  
11  
12 5 investigations cannot always be avoided, there is enormous potential to mine Google  
13  
14 6 Earth across different space and time scales, supporting the assembly of large,  
15  
16 7 reliable data sets relevant to river forms and processes in a very cost-effective way.  
17  
18  
19 8

## 9 **KEYWORDS**

10 Google Earth, form, process, geomorphic units, river classification

## 1 INTRODUCTION

### 2 **Google Earth as a potential information source for investigating river forms and** 3 **processes**

4 Bizzi et al. (2015) and Marcus and Fonstad (2010) reviewed the many possibilities for  
5 supporting research relevant to river science and management that are offered by  
6 advances in remote sensing technologies and data analysis techniques, and the  
7 increasing availability of remotely sensed data sets. They concluded that data  
8 acquisition costs remain relatively high and data processing usually requires  
9 significant expertise, with the result that the use of remote sensing data in river science  
10 continues to be focused on resolving specific questions and developing sophisticated  
11 modelling methodologies (e.g. Alber and Piégay, 2011; Schmitt et al., 2014), usually  
12 in relation to particular geographical areas of interest. However, Google Earth is  
13 highlighted as a freely available global information system that provides a range of  
14 remotely-sensed data sets in a format that can be easily used by river scientists and  
15 practitioners who have little background in remote sensing. Thus, Google Earth  
16 provides some potential for exploiting remotely sensed data more widely within river  
17 science and management (e.g. Large and Gilvear, 2015).

18  
19 Google Earth incorporates a virtual globe based on the World Geodetic System 1984  
20 (WGS 1984) onto which geographical information is projected. Data layers include  
21 satellite and aerial images which are georeferenced to the same virtual globe. The  
22 typical baseline resolution of Google Earth data varies across the Earth's surface  
23 according to the imagery incorporated within the information system. Across Europe,  
24 the study area for the research reported herein, recent images are often of high spatial  
25 resolution because of the wide availability of airborne imagery with resolutions of 0.15-

1  
2  
3 1 0.30 m. Where imagery is acquired by satellite, the resolution varies from  
4  
5 2 approximately 0.3-0.5 m (Digital Globe's WorldView platform) to 10-30 m (ESA's  
6  
7 3 Sentinel 2 and NASA's Landsat 8). Historical imagery (usually extending back to ca.  
8  
9 4 2000, but sometimes to the mid-twentieth century) is also available for most locations.  
10  
11 5 In addition, digital elevation data from NASA's Shuttle Radar Topography Mission  
12  
13 6 (SRTM, Farr et al., 2007) are incorporated into Google Earth and the data can be  
14  
15 7 extracted as point elevations. Google Earth therefore represents a potentially  
16  
17 8 significant source of information to support many environmental investigations  
18  
19 9 because it is freely available, it integrates a vast selection of images as well as digital  
20  
21 10 elevation data, and it provides tools to extract elevation and distance measurements.  
22  
23  
24  
25  
26  
27  
28

## 29 12 **Morphological classification of rivers**

30  
31 13 The physical attributes (i.e. size, shape, bed and bank materials, constituent  
32  
33 14 geomorphic/habitat features) and behavioural characteristics (i.e. magnitude,  
34  
35 15 frequency and style of adjustment, sensitivity) of rivers are determined by controls that  
36  
37 16 operate over a range of spatial and temporal scales (Brierley and Fryirs, 2005). For  
38  
39 17 example, lithology and tectonic setting influence both the potential energy available to  
40  
41 18 a river to perform geomorphic work (via their effect on elevation, slope and valley  
42  
43 19 width) and the amount and type of sediment available for transport. Likewise, climate  
44  
45 20 (both directly and indirectly through its control on vegetation) influences the  
46  
47 21 magnitude, frequency and sequencing of flow and sediment transport. Spatial variation  
48  
49 22 in these boundary conditions along and between rivers gives rise to different process  
50  
51 23 interactions that combine to produce remarkable reach-scale diversity in terms of river  
52  
53 24 appearance and responses to individual flood events.  
54  
55  
56  
57  
58  
59  
60

1  
2  
3 1 This fundamental link between form and process has provided the theoretical basis  
4  
5 2 upon which numerous river classification schemes have been developed (e.g.  
6  
7 3 Schumm, 1977; Montgomery and Buffington, 1997; Brierley and Fryirs, 2005; Beechie  
8  
9 4 et al., 2006; Gurnell et al., 2016). Such classifications share a common goal of seeking  
10  
11 5 to simplify the complexity of natural landscapes by identifying locations that function  
12  
13 6 in similar ways (Tadaki et al., 2014; Kondolf et al., 2016), thereby providing a spatial  
14  
15 7 framework under which, for example, links between physical and ecological processes  
16  
17 8 can be investigated (Frissell et al., 1986; Naiman, 1998), hypotheses regarding the  
18  
19 9 impacts of landscape disturbance can be developed and tested (Buffington and  
20  
21 10 Montgomery, 2013), reaches suitable for rehabilitation can be identified (Brierley and  
22  
23 11 Fryirs, 2000), and river restoration designs can be developed and implemented  
24  
25 12 (Rosgen, 1994). This is achieved through the measurement of a variety of physical  
26  
27 13 properties (increasingly quantified across different scales), selected on the basis that  
28  
29 14 they are somehow reflective of the underlying processes that determine the  
30  
31 15 appearance and behaviour of the river at a given point.  
32  
33  
34  
35  
36  
37  
38  
39

40 17 There has been considerable debate over the appropriateness of certain river  
41  
42 18 classification schemes for applications in river management (Simon et al., 2007; Lave,  
43  
44 19 2009), with criticism centred on their lack of direct measurement of process rates,  
45  
46 20 together with insufficient recognition of the importance of catchment and historical  
47  
48 21 context (Montgomery and Buffington, 2013). Nevertheless, recent analysis by Kasprak  
49  
50 22 et al. (2016) has shown that there can be widespread agreement between the outputs  
51  
52 23 of different classification frameworks that have varying degrees of sophistication and  
53  
54 24 data requirements when applied in the same catchment, suggesting some of these  
55  
56 25 concerns may be overstated and that meaningful inference of fluvial processes can be  
57  
58  
59  
60

1 achieved through relatively straightforward quantification of form-based parameters.  
2 While this is encouraging, the vast majority of existing classification schemes are  
3 difficult to apply in situations where field measurement is dangerous and/or  
4 impractical, secondary data on channel morphology, grain size, etc. are either not  
5 available or spatially limited, and/or a large number of rivers need to be classified.  
6 They also fail to take full advantage of the improved variety and coverage of  
7 geomorphologically-relevant data that emerging technologies are generating. Google  
8 Earth provides an enormous, freely available data source that could be exploited for  
9 investigating many aspects of river environments; this research specifically explores  
10 whether it can support discrimination of river types through the extraction of form-  
11 based process indicators.

### 13 **Research aims**

14 In this paper, we explore the degree to which data sets describing process-relevant  
15 dimensional and morphological characteristics of rivers can be extracted from Google  
16 Earth via its Google Earth Pro software application. We test the utility of this  
17 information by investigating whether it can be used to develop a geomorphologically-  
18 meaningful, empirically-based classification of European semi-natural rivers,  
19 focussing mainly on single thread and transitional river planform styles. Our  
20 empirically-based analysis is bottom-up, allowing observed form-based process  
21 indicators to drive the classification rather than applying any *a priori* discrimination  
22 rules (for example, differentiating between river reaches on the basis of a  
23 predetermined sinuosity threshold). We then test the outcomes of the classification by  
24 examining the characteristics and distribution of the river classes identified through  
25 our analysis in relation to known independent controls of river form including reach-

1  
2  
3 1 scale energy and valley confinement conditions, thereby exploring the extent to which  
4  
5 2 process can be inferred from form.  
6  
7  
8 3

## 10 4 **METHODS**

### 12 5 **Reach selection**

14 6 In order to test the degree to which meaningful morphological features and dimensions  
15  
16 7 can be extracted from Google Earth, sites displaying single thread or transitional  
17  
18 8 planform styles (the planform types that dominate in Europe, Tockner et al., 2009)  
19  
20 9 were selected for analysis which were also:  
21  
22  
23  
24 10

26 11 (i) as morphologically intact and free to adjust as possible. This was achieved by  
27  
28 12 identifying river sites that appeared to be unconfined by buildings, infrastructure and  
29  
30 13 channel training works such as embankments. Because of the widespread  
31  
32 14 modification of European rivers, sites where up to 10 % of the channel length was  
33  
34 15 affected by engineering structures were permitted, although virtually all selected sites  
35  
36 16 showed a negligible extent of such interventions. However, it is important to note that  
37  
38 17 not all modifications are apparent from a planview image and thus some selected sites  
39  
40 18 may have greater modification than was anticipated;  
41  
42  
43  
44 19

46 20 (ii) located at sites with unregulated flow regimes. All sites displayed little evidence of  
47  
48 21 large dams upstream, although one was located downstream of what appeared to be  
49  
50 22 a large natural lake and another was close to an upstream weir. However, evidence  
51  
52 23 of considerable flow and sediment dynamics in the sequence of available images  
53  
54 24 suggested that this structure was probably quite low and/or imposed minimal flow and  
55  
56 25 sediment regulation on downstream reaches. Most sites were located within 30 km of  
57  
58  
59  
60



1  
2  
3 1 a river flow gauging station that had been deemed to have a near-natural flow regime  
4  
5 2 (Stahl et al., 2010). The list of gauging stations emanated from a European research  
6  
7 3 programme (FRIEND) that did not include all countries within Europe. As a result, not  
8  
9 4 all European countries were represented among the selected sites and only a few sites  
10  
11 5 were included from countries that were not part of the FRIEND programme;  
12  
13  
14  
15  
16

17 7 (iii) represented by at least one cloud free, high resolution image since 2000, which  
18  
19 8 appeared to show the river under baseflow conditions to maximise the potential to  
20  
21 9 identify in-channel features.  
22  
23

24 10

25  
26 11 These reach selection criteria were designed to ensure that, as far as practically  
27  
28 12 possible, morphological features and dimensions could a) be easily identified and b)  
29  
30 13 would be reflective of a process regime not significantly affected by anthropogenic  
31  
32 14 activity. 68 suitable sites were identified (Figure 1) on different European rivers and up  
33  
34 15 to three reaches (each with a length exceeding 70 active widths) were selected for  
35  
36 16 analysis within each site, giving a total of 194 reaches from which dimensional and  
37  
38 17 morphological information could be extracted. A minimum reach length of 70 active  
39  
40 18 widths was used to maximise opportunities for feature identification and reduce the  
41  
42 19 effect of any vertical inaccuracy in elevation data on derived slope values. The mean  
43  
44 20 reach length was 7.2 km.  
45  
46  
47  
48

49 21

## 50 22 **Feature extraction and processing**

51  
52 23 A list of channel dimensions and associated indices (Table 1) and morphological  
53  
54 24 features (Table 2) was assembled that had both process relevance and the potential  
55  
56 25 to be extracted from Google Earth imagery and digital elevation data. Rules for feature  
57  
58  
59  
60

1  
2  
3 1 identification were developed iteratively by inspecting images of many river reaches  
4  
5 2 until a stable set of features and identification rules was established. This set of  
6  
7 3 features was then extracted for each of the 194 reaches.  
8  
9  
10 4

11  
12 5 Morphological feature frequency is affected by the dimensions of the river reach in  
13  
14 6 which the features are located, including the reach length (the longer the length, the  
15  
16 7 greater the expected number of any particular feature) and also river width (the wider  
17  
18 8 the river, the smaller the expected number of any particular feature within a particular  
19  
20 9 length of reach). Therefore, morphological feature frequency measurements were  
21  
22 10 standardised to allow for the size of each sampled reach by multiplying each feature  
23  
24 11 frequency by the ratio of active channel width to active reach length.  
25  
26  
27  
28  
29  
30  
31  
32

33 13 When extracting river dimensions and features at each site, the available images were  
34  
35 14 inspected and the image that appeared to represent the lowest flow was typically used  
36  
37 15 for the feature count. However, in some cases other criteria had to be considered.  
38  
39 16 Cloud cover or heavy shading sometimes obscured significant lengths of river, in  
40  
41 17 which case an alternative image or both images were used for feature extraction. In  
42  
43 18 addition, a few reaches had been recently affected by engineering interventions and  
44  
45 19 so earlier, pre-intervention images were used for feature extraction.  
46  
47  
48  
49

### 50 21 **Classification of river reaches**

51 22 Principal Components Analysis (PCA) was used to investigate the nature of any  
52  
53 23 channel dimensional and morphological gradients present in the 194 reach data set.  
54  
55 24 PCA was performed on a Spearman's  $\rho$  correlation matrix and a varimax rotation with  
56  
57 25 Kaiser normalisation was applied to the set of PCs with eigenvalues greater than one,  
58  
59  
60

1  
2  
3 1 to align them as closely as possible to the original variables and thus aid interpretation  
4  
5 2 of the environmental gradients that the PCs described. Correlation coefficients for  
6  
7 3 pairs of input variables and the results of Kaiser-Meyer-Olkin and Bartlett's sphericity  
8  
9 4 tests were examined prior to PCA to ensure the selection of variables was robust and  
10  
11 5 sampling was adequate.  
12  
13  
14  
15  
16

17 7 Agglomerative hierarchical clustering (AHC) using Ward's algorithm was then applied  
18  
19 8 to the reach scores on the varimax-rotated PCs. Reaches were assigned to different  
20  
21 9 classes according to a natural break in the dendrogram based on the entropy level.  
22  
23 10 The distinctiveness of the resultant reach class clusters was then validated statistically  
24  
25 11 using Kruskal-Wallis (KW) tests followed by multiple pairwise comparisons, based on  
26  
27 12 Dunn's procedure with Bonferroni correction. Qualitative descriptions of each class of  
28  
29 13 river were then developed through examination of trends in bi-plots of reach PC scores  
30  
31 14 and the results of the pairwise comparisons. All analyses were conducted using the  
32  
33 15 2018 version of XLSTAT Pro (<http://www.addinsoft.com>).  
34  
35  
36  
37  
38  
39

### 40 17 **Geomorphological 'realism' of the classification**

41  
42 18 The degree to which the classification enabled discrimination of reaches subject to  
43  
44 19 different process regimes was evaluated through examination of the distribution of  
45  
46 20 reaches in each class in relation to variables describing known independent controls  
47  
48 21 of river morphology and behaviour. Local energy conditions (as a proxy for sediment  
49  
50 22 transport capacity and potential for morphological adjustment) were represented using  
51  
52 23 a combination of valley slope (calculated using reach elevation data and valley length  
53  
54 24 measurements from Google Earth) and a representative flood discharge. Valley slope  
55  
56 25 was used instead of a measure of channel slope (e.g. Leopold and Wolman, 1957) as  
57  
58  
59  
60

1  
2  
3 1 it is independent of channel sinuosity and, thus, river class (Ferguson, 1984; 1987).  
4  
5 2 For the majority of reaches (145), long flow gauging station records (>19 years in most  
6  
7 3 cases) were available to estimate the two-year return period flood discharge ( $Q_2$ ). This  
8  
9 4 hydrological parameter was selected on the basis that it is also independent of channel  
10  
11 5 morphology (van den Berg, 1995). Bankfull discharge has been commonly used as an  
12  
13 6 explanatory variable in studies of river pattern (e.g. Leopold and Wolman, 1957) as it  
14  
15 7 is considered to approximate the dominant (or effective) discharge that is theoretically  
16  
17 8 representative of the full range of flows that determine sediment transport and  
18  
19 9 morphological configuration in a given channel (Hey and Thorne, 1986). However, it  
20  
21 10 is sensitive to changes in width:depth ratio (and, therefore, river class), is routinely  
22  
23 11 estimated in a number of different ways and is not readily available at many locations  
24  
25 12 (van den Berg, 1995). For a small number of reaches where flow data were not  
26  
27 13 available, a literature-sourced estimate of the bankfull discharge was used as a  
28  
29 14 substitute on the basis that it is comparable in magnitude to  $Q_2$  for many rivers  
30  
31 15 (Knighton, 1998).  
32  
33  
34  
35  
36  
37  
38  
39

40 17 Following Kleinhans and van den Berg (2011), these variables were combined to  
41  
42 18 compute a potential specific stream power ( $W\ m^{-2}$ ),  $\omega_{pv}$ , designed to represent the  
43  
44 19 energy available to perform geomorphic work in a given reach (Ferguson, 1987):  
45  
46  
47  
48

$$21 \quad \omega_{pv} = \frac{\rho g Q S_v}{W_r} \quad (1)$$

52 22  
53  
54 23 where  $\rho$  = water density ( $kg\ m^{-3}$ ),  $g$  = acceleration due to gravity ( $m\ s^{-2}$ ),  $Q$  = reference  
55  
56 24 discharge ( $m^3\ s^{-1}$ ) (two year return period flood or bankfull discharge),  $S_v$  = valley slope  
57  
58 25 ( $m\ m^{-1}$ ) and  $W_r$  = reference channel width (m). A reference, rather than actual, width  
59  
60

1 is used in the calculation so as to remain independent of channel type (see van den  
2 Berg, 1995, and Kleinhans and van den Berg, 2011, for detailed discussion of the  
3 merits of this approach). It is calculated using a regime equation:

$$W_r = \alpha \sqrt{Q} \quad (2)$$

4  
5  
6  
7 with a coefficient of  $\alpha = 3.0 \sqrt{s m^{-1}}$  used in this application (Kleinhans and van den  
8 Berg, 2011).

9  
10 The computation of  $\omega_{pv}$  allowed the relationship between local energy conditions and  
11 descriptors of channel morphology (e.g. active channel width, sinuosity, etc.) derived  
12 from Google Earth to be explored. Previous research (Antropovskiy, 1972, cited in  
13 Alabyan and Chalov, 1998; van den Berg, 1995; Bledsoe and Watson, 2001;  
14 Kleinhans and van den Berg, 2011) has demonstrated that channel-independent  
15 measures of stream power can prove effective in discriminating between, and  
16 supporting interpretation of, different types of meandering and braided channels when  
17 bed material grain size is accounted for. The distribution of a subset of river reaches  
18 classified in this study (for which grain size data were available) was evaluated in  
19 relation to the following channel type discriminators from this published work:

$$\omega_{bm} = 900 D_{50}^{0.42} \quad (3)$$

20  
21  
22  
23 where  $D_{50}$  = median bed material grain size (m) and  $bm$  refers to a threshold between  
24 highly braided and meandering channels (van den Berg, 1995);

$$\omega_{sc} = 285 D_{50}^{0.42} \quad (4)$$

where *sc* refers to a threshold between active meandering channels that exhibit scroll bars and those which exhibit chute (and scroll) bars (Kleinhans and van den Berg, 2011); and

$$\omega_{ia} = 90 D_{50}^{0.42} \quad (5)$$

where *ia* refers to a threshold between laterally inactive channels and active meandering channels with scroll bars (Makaske et al., 2009).

Elevation and valley confinement conditions (as proxies for the potential significance of colluvial processes and restrictions on lateral mobility) were also quantified. Reach elevation was measured directly from Google Earth at the upstream boundary. Level of confinement was approximated by the proportion of the bank length that appeared to be in contact with valley side slopes and any high (ancient) terraces: reaches were deemed to be confined when more than 90% of the river bank length was in contact; unconfined when less than 10% of their river bank length was in contact; and partly confined where an intermediate level of bank contact was evident (Brierley and Fryirs, 2005).

## RESULTS

### Classification and characteristics of river reaches

Principal Components Analysis was performed on a Spearman's rank correlation matrix for 13 variables (Tables 1 and 2). Four variables represented river channel

1  
2  
3 1 dimensions: active channel sinuosity, the ratio of baseflow to active channel sinuosity,  
4  
5 2 the ratio of median active to median baseflow channel width, the coefficient of variation  
6  
7  
8 3 of active channel width. These variables were selected to illustrate the planform  
9  
10 4 character of the river reaches independently from their size. The remaining nine  
11  
12 5 variables were counts of the physical features listed in Table 2 once they had been  
13  
14  
15 6 standardised for the length and width of the active channel.  
16  
17 7

18  
19 8 The first four PCs all had eigenvalues greater than 1, indicating that they explained  
20  
21 9 more of the variance in the data set than the original variables (Table 3). A varimax  
22  
23  
24 10 rotation of these four PCs simplified the structure of the loadings matrix and supported  
25  
26 11 interpretation of the environmental gradients that they described. Focussing mainly on  
27  
28 12 those variables with loadings  $\geq 0.7$  (Table 3), PC1 describes a gradient from reaches  
29  
30  
31 13 with little variation in width or sinuosity with increasing flow stage (positive loadings of  
32  
33 14 0.827 on Active:Baseflow channel width and 0.816 on Baseflow:Active channel  
34  
35 15 sinuosity, respectively) and also limited longitudinal variability in their width (positive  
36  
37 16 loading of 0.692 on Coefficient of variation of active channel width), to those with active  
38  
39 17 channels that are distinctly wider and less sinuous than their baseflow channels,  
40  
41  
42 18 containing increasing numbers of active lateral and mid channel bars (positive  
43  
44 19 loadings of 0.910 on Active lateral bar and 0.800 on Active mid-channel bar,  
45  
46 20 respectively). The remaining three PCs describe gradients of increasing frequency of  
47  
48  
49 21 Active point bars and Channel cutoffs (PC2), increasing frequency of Bedrock and  
50  
51  
52 22 Rapids (PC3), and increasing frequency of Cascades and Steps (PC4). Finally,  
53  
54 23 although the loading is relatively weak (-0.614), Riffles show a negative loading on  
55  
56 24 PC4.  
57  
58  
59 25

1  
2  
3 1 Agglomerative hierarchical clustering on the reach PC scores using Ward's algorithm  
4  
5 2 and an entropy-based solution resulted in the identification of five clusters, each  
6  
7 3 representing a different class of river reach (Figure 2). Classes A and B were found to  
8  
9 4 be most similar in terms of their characteristics and, together with class C reaches,  
10  
11 5 formed a higher level grouping that was dissimilar from classes D and E. Kruskal-  
12  
13 6 Wallis tests followed by multiple pairwise comparisons, based on Dunn's procedure  
14  
15 7 with Bonferroni correction, were used to establish which clusters showed significant  
16  
17 8 differences in their scores on each of the PCs (Table 4). All five clusters were found  
18  
19 9 to be fully discriminated by these analyses, with each cluster showing a significant  
20  
21 10 difference from the others in relation to the scores on at least one PC. The distribution  
22  
23 11 of the five classes with respect to the four PCs is illustrated in Figure 3. There is  
24  
25 12 separation of classes B, C and E from class A along PC1 (Figure 3A) and class D from  
26  
27 13 the other classes along PC 3 (Figure 3B). Furthermore, class B is discriminated from  
28  
29 14 the other classes by PC2 (Figure 3C) and, apart from a group of outliers in class D,  
30  
31 15 class E is distinguished from the other classes by PC4 (Figure 3D).  
32  
33  
34  
35  
36  
37  
38  
39

40 17 Based on the variables with high loadings on each PC (Table 3) and significant  
41  
42 18 differences identified between the scores of reaches within the five classes on each  
43  
44 19 PC (Table 4), Table 5 provides a summary interpretation of the five classes, along with  
45  
46 20 an example reach from the centre of each cluster for visualisation purposes. In more  
47  
48 21 detail, the classes are interpreted as follows:  
49  
50  
51  
52  
53

54 23 Class A: Laterally stable channels with an absence of visible instream depositional  
55  
56 24 features, and very limited variability in either width or sinuosity with increasing flow  
57  
58 25 stage, or in width along their length.  
59  
60



1  
2  
3 1  
4  
5 2 Class B: Laterally active sinuous-meandering channels with visible point bars and  
6  
7 3 cutoffs that become wider and less sinuous with increasing flow stage, and which vary  
8  
9 4 in active width along their length.  
10  
11  
12 5

13  
14 6 Class C: Transitional (near-braided) channels with visible lateral and/or mid-channel  
15  
16 7 bars with intervening riffles, which become wider and less sinuous with increasing flow  
17  
18 8 stage, and which vary in width along their length.  
19  
20 9

21  
22  
23 10 Class D: Bedrock channels with visible rapids and, in some cases, cascade and/or  
24  
25 11 step features. Low to intermediate variation in channel width or sinuosity with flow  
26  
27 12 stage and the presence of occasional bars.  
28  
29 13

30  
31  
32 14 Class E: Cascade/step dominated channels with occasional lateral and/or mid-  
33  
34 15 channel bars and an absence of visible point bars, riffles and exposed bedrock.  
35  
36 16 Intermediate to strong variation in width both longitudinally and with increasing flow  
37  
38 17 stage.  
39  
40 18

#### 41 42 43 44 19 **Relationships between channel morphology and independent control variables**

45  
46 20 The relative frequencies of fully, partly and unconfined reaches in each of the five river  
47  
48 21 classes are shown in Figure 4. The majority of laterally stable and laterally active  
49  
50 22 sinuous-meandering reaches (classes A and B) are unconfined (85% and 97%,  
51  
52 23 respectively), with the remainder being partly confined. The valley confinement  
53  
54 24 settings of transitional channel (class C) reaches are more varied, with 51% being  
55  
56 25 unconfined, 38% partly confined and 10% fully confined. Bedrock channels (class D)

1 and, particularly, cascade/step dominated (class E) reaches are typically located in  
2 fully confined valley settings, accounting for 55% and 73%, respectively, of each class.  
3 Amongst bedrock channel (class D) reaches, 20% are in partly confined valley settings  
4 and 25% are unconfined. In comparison, only 7% of cascade/step dominated (class  
5 E) reaches are unconfined, with the remainder (20%) located in partly confined valley  
6 settings.

7  
8 Cascade/step dominated (class E) reaches are situated at significantly higher  
9 elevations (all greater than 500 m and the majority above 1000 m) than reaches in the  
10 other four classes (Figure 5). Laterally stable (class A) and laterally active sinuous  
11 meandering (class B) reaches tend to be found at much lower elevations (median =  
12 92 m and 133 m, respectively). The average height of transitional (class C) and  
13 bedrock (class D) channel reaches is similar (median = 277 m and 124 m, respectively)  
14 but reaches in these classes occupy a wider range of elevations from near sea-level  
15 up to approximately 1000 m and 2300 m, respectively.

16  
17 The distribution of reaches in the five river classes with respect to  $Q_2$  and valley slope  
18 is illustrated in Figure 6. There is notable overlap between some of the classes,  
19 particularly for transitional (class C) and bedrock (class D) channels, but others occupy  
20 relatively discrete areas of the plot. Cascade/step dominated (class E) reaches are  
21 grouped in the upper left region of the plot, with contrasting high valley slopes but  
22 relatively low discharges. Bedrock channel (class D) reaches tend to occupy the centre  
23 and right of the plot, with relatively high slopes or high discharges, in a similar zone to  
24 most of the transitional channel (class C) reaches. The bottom left region of the plot is  
25 exclusively occupied by laterally stable (class A) reaches, which persist with increasing

1  
2  
3 1 slope and/or discharge towards the centre. Laterally active sinuous-meandering (class  
4  
5 2 B) reaches occupy a zone that combines intermediate slope and discharge.  
6  
7  
8 3

9  
10 4 Figure 7 illustrates the range of potential specific stream power values of reaches of  
11  
12 5 different classes for which an estimate of bed material grain size was available and  
13  
14 6 shows their distribution relative to empirically-derived thresholds between alluvial  
15  
16 7 channels types derived using Equations 3-5. Laterally stable (class A) reaches occur  
17  
18 8 at a wide range of potential specific stream powers, existing under conditions where  
19  
20 9 no lateral movement or bar formation would be expected but also those potentially  
21  
22 10 capable of instigating scroll and chute bar development and even active braiding.  
23  
24 11 Transitional (class C) channels are almost exclusively restricted to a range of potential  
25  
26 12 specific stream power values above the threshold required for meandering with scroll  
27  
28 13 and chute bar development and moderate braiding but below that required for  
29  
30 14 significant levels of braiding. Laterally active sinuous-meandering (class B) reaches  
31  
32 15 span a domain above the potential specific stream power threshold required for scroll  
33  
34 16 bar development but below that above which highly braided rivers occur.  
35  
36  
37  
38  
39  
40  
41

42 18 Figures 8a and 8b highlight the existence of complex associations, at class level,  
43  
44 19 between potential specific stream power and morphological parameters (channel  
45  
46 20 width and sinuosity) typically used in other classifications but which did not explicitly  
47  
48 21 inform the groupings identified above. The active widths of laterally stable (class A)  
49  
50 22 channels tend to be narrower than those of laterally active sinuous meandering (class  
51  
52 23 B) and transitional (class C) reaches for a given potential specific stream power. The  
53  
54 24 active channels of cascade/step dominated (class E) reaches are relatively narrow in  
55  
56 25 comparison to reaches from other classes apart from laterally stable (class A)  
57  
58  
59  
60

1  
2  
3 1 channels, albeit at much greater potential specific stream powers, while the active  
4  
5 2 widths of bedrock (class D) channels are more variable. A general trend of declining  
6  
7 3 active channel sinuosity with increasing potential specific stream power is evident from  
8  
9 4 laterally active sinuous-meandering (class B), through transitional (class C) and  
10  
11 5 bedrock (class D), to cascade/step dominated (class E) channel reaches. However,  
12  
13 6 laterally stable (class A) channels exhibit a wide range of sinuosity values that appear  
14  
15 7 to be unrelated to local energy conditions.  
16  
17  
18  
19  
20  
21  
22  
23

## 24 9 **DISCUSSION**

### 25 10 **Extraction of geomorphologically-relevant information from Google Earth** 26 11 **images**

27  
28 12 Our analysis of information extracted from Google Earth Pro has yielded a  
29  
30 13 classification of river types that not only appears geomorphologically-intuitive but  
31  
32 14 confirms previously hypothesised associations with independent data sets that  
33  
34 15 describe a set of controlling variables. Nevertheless, there are a number of issues that  
35  
36 16 constrain how far and at what resolutions geomorphologically-relevant data can be  
37  
38 17 extracted from Google Earth.  
39  
40  
41  
42  
43  
44  
45  
46  
47  
48  
49  
50  
51  
52  
53  
54  
55  
56  
57  
58  
59  
60

19 The level of detail achieved by the geomorphological classification of European rivers  
20 presented herein is largely determined by the types of process indicators that can be  
21 resolved from Google Earth images and the accuracy with which they can be  
22 measured or counted. The potential significance of these factors is a function of the  
23 number, timing and resolution of the available images in the Google Earth database  
24 for a given reach. An expanded list of potential process indicators was originally  
25 considered for the study, including a more comprehensive suite of bar types,

1  
2  
3 1 vegetation types and associated morphological units including benches, and instream  
4  
5 2 assemblages of large wood. This could, in theory, have led to the isolation of further  
6  
7 3 groupings or sub-types of reaches but these features proved difficult to reliably identify  
8  
9  
10 4 as a result of the lack of control on flow stage and/or season at the time of image  
11  
12 5 capture, water clarity issues and/or obscuration by riparian trees. Wherever possible,  
13  
14 6 we worked on images that appeared to represent baseflow conditions, but of course  
15  
16 7 we cannot be sure that we had acceptably comparable flow levels in all of the images  
17  
18 8 we analysed. This was a particular issue where the number of clear images was small,  
19  
20 9 since this prevented comparisons to confirm differences in stage. This issue  
21  
22 10 underpinned our decision to rely more heavily on active channel dimensions in our  
23  
24 11 analysis, since these were more consistently identified using the edge of continuous  
25  
26 12 vegetation cover as the criterion. In addition, where only summer images could be  
27  
28 13 analysed or where image resolution was low, riparian vegetation could have adversely  
29  
30 14 affected all data extraction, but particularly the identification of smaller or more  
31  
32 15 nuanced in-channel physical features.  
33  
34  
35  
36  
37  
38  
39

40 17 The procedures for identifying and measuring or counting the process indicators  
41  
42 18 utilised in this study were completed manually. The pan, zoom and path measurement  
43  
44 19 tools available in Google Earth Pro make this a relatively straightforward task but it is  
45  
46 20 time-consuming to complete for a large sample of river reaches and introduces the  
47  
48 21 potential for human error. Recent developments in image processing technology and  
49  
50 22 increasing provision of freely-available remotely sensed data products could facilitate  
51  
52 23 the semi- or complete automation of the geomorphological classification approach  
53  
54 24 proposed in this paper. The release of Google's Earth Engine cloud computing  
55  
56 25 platform in 2010 has provided the research community with both access to remotely  
57  
58  
59  
60

1  
2  
3 1 sensed imagery and the computational power required to process such data at the  
4  
5 2 global scale (Gorelick et al., 2017). It has enabled analyses with a spatial and temporal  
6  
7 3 richness that would previously have been considered unachievable, including tracking  
8  
9 4 surface water dynamics (Pekel et al., 2016), quantifying the status and distribution of  
10  
11 5 sensitive habitats (Giri et al., 2010) and monitoring urban development (Patel et al.,  
12  
13 6 2015). To date, this research has largely been centred on the use of data from NASA's  
14  
15 7 Landsat and ESA's Copernicus programmes but neither platform offers the spatial  
16  
17 8 resolution necessary to resolve the types of features used in this study. However, this  
18  
19 9 situation is changing with the emergence of increasingly high resolution geospatial  
20  
21 10 data products. The recent release of Planet's SkySat imagery via Google Earth  
22  
23 11 Engine, offering true colour imagery at sub-metre resolution and multispectral imagery  
24  
25 12 at 2 m resolution, could enable the accurate automated delineation of channel  
26  
27 13 boundaries and geomorphic units. The process of identifying and extracting  
28  
29 14 geomorphologically-relevant information from this high resolution imagery would not  
30  
31 15 be an insignificant task but comprehensive taxonomic frameworks for the identification  
32  
33 16 of a huge range of fluvial landforms already exist (e.g. Wheaton et al., 2015), image  
34  
35 17 processing workflows capable of extracting channel networks and their geometric  
36  
37 18 properties have been developed (e.g. Isikdogan et al., 2017; Monegaglia et al., 2018),  
38  
39 19 and object-based image analysis techniques have great potential for identifying  
40  
41 20 spatially-distinctive features (e.g. Demarchi et al., 2016; Demarchi et al., 2017). We  
42  
43 21 encourage further research towards the goal of operationalising such methods for  
44  
45 22 global application in the field of river classification.  
46  
47  
48  
49  
50  
51  
52  
53  
54  
55

## 56 **Geomorphological 'realism' of the classification**

57  
58  
59  
60

1  
2  
3 1 We have explored the utility of Google Earth as a source of geomorphologically-  
4  
5 2 relevant information by developing a classification of transitional to single thread near-  
6  
7 3 natural European rivers. The apparent 'realism' of this classification is one test of the  
8  
9 4 utility of the extracted data on which it is based, but the classification is also dependent  
10  
11 5 upon a number of other factors.  
12  
13 6

14  
15 6  
16  
17 7 In addition to being influenced by the nature of data available through Google Earth,  
18  
19 8 the reach types identified in this study were also determined to a certain degree by the  
20  
21 9 sampling strategy employed. Our focus was on river reaches whose morphology was  
22  
23 10 considered to be "in tune" with a natural process regime (i.e. not visibly affected by  
24  
25 11 dams or other engineering activities). This immediately precluded many lowland  
26  
27 12 systems from our analysis given their long history of management in Europe and, as  
28  
29 13 a result, prevented the inclusion of a number of possible additional process indicators  
30  
31 14 such as stable (vegetated) islands as they would have been present in such low  
32  
33 15 quantities across the sample of 194 reaches that their inclusion would have  
34  
35 16 compromised the PCA undertaken. The same is true of natural large braided rivers,  
36  
37 17 which were once common across the Alps and other mountainous regions of Europe  
38  
39 18 but have been heavily impacted by flow regulation, gravel extraction and erosion  
40  
41 19 control measures (Tockner et al., 2003). Together, this accounts for the absence of  
42  
43 20 several "classic" river types (e.g. anastomosing, fully braided, etc.) that would  
44  
45 21 potentially have emerged from the classification procedure had it been undertaken on  
46  
47 22 rivers in other parts of the world.  
48  
49  
50  
51  
52  
53  
54  
55

56 24 It is also important to acknowledge that, despite our best efforts to only sample river  
57  
58 25 reaches that did not have any obvious artificial constraints on their adjustment for  
59  
60

1  
2  
3 1 analysis, this is not straightforward when working with planview aerial imagery. In  
4  
5 2 particular, bank reinforcement is rarely visible in these data products. Therefore, we  
6  
7 3 cannot be sure that significant reinforcement was not in place, and on the larger,  
8  
9 4 lowland rivers it is likely to have been present to some extent. In addition, in the few  
10  
11 5 reaches where cross-channel structures were present, we ensured that they were  
12  
13 6 limited in number but their vertical extent and thus potential impact on upstream and  
14  
15 7 downstream dynamics could not be assessed. The presence of engineered structures  
16  
17 8 in individual reaches may have influenced the recorded process indicator values through  
18  
19 9 their impacts on hydraulic and sediment transport processes and, thus, may have  
20  
21 10 affected the allocation of reaches to particular classes.  
22  
23  
24  
25  
26  
27  
28  
29  
30  
31  
32  
33  
34  
35  
36  
37  
38  
39  
40  
41  
42  
43  
44  
45  
46  
47  
48  
49  
50  
51  
52  
53  
54  
55  
56  
57  
58  
59  
60

12 Despite these caveats, the classification procedure resulted in the definition of five  
13 river reach types with distinctive geomorphological identities whose internal  
14 characteristics and distribution can be explained in relation to known independent  
15 controls on river form. Under low energy conditions in unconfined valley settings,  
16 laterally stable channels lacking visible instream depositional features and longitudinal  
17 variation in width, and which do not experience significant changes in width or sinuosity  
18 with increasing flow stage, were found to dominate. These reaches tended to be  
19 relatively narrow in comparison to the other reach types found in unconfined settings.  
20 Such characteristics are consistent with those of suspended load-dominated channels  
21 with relatively low width-depth ratios and banks formed of highly resistant cohesive  
22 sediments. Under increasingly energetic conditions (but remaining in unconfined  
23 settings), reaches with those characteristics were still observed but became less  
24 common relative, firstly, to laterally active sinuous-meandering channels and then, at  
25 even greater values of  $\omega_{vp}$ , transitional (near-braided) channels. The fact that laterally



1  
2  
3 1 stable channels are able to persist under high energy conditions is perhaps initially  
4  
5 2 surprising but it is important to remember that it is the strength of the erosive force  
6  
7 3 relative to the resistive strength of the boundary that ultimately determines channel  
8  
9 4 mobility (Huang et al., 2004). Closer visual inspection of a sample of laterally stable  
10  
11 5 reaches at the upper end of the energy gradient revealed the presence of mature  
12  
13 6 riparian trees along their banks. Riparian vegetation can be highly effective in  
14  
15 7 increasing the stability of river banks through both its effect on near-bank hydraulic  
16  
17 8 roughness (Tooth and McCarthy, 2004) and by binding sediments together (Holloway  
18  
19 9 et al., 2017). These processes or, potentially, the presence of undetected bank erosion  
20  
21 10 control structures may explain the occurrence of this type of reach under high energy  
22  
23 11 conditions.  
24  
25  
26  
27  
28  
29  
30

31 13 The occurrence of laterally active sinuous-meandering reaches with visible point bars  
32  
33 14 and cutoff features that vary longitudinally in width and become wider and less sinuous  
34  
35 15 with increasing flow stage was found to be consistent with situations where local  
36  
37 16 hydraulic conditions are sufficiently energetic to mobilise bedload material and  
38  
39 17 overcome the resistive strength of the channel boundary. When bed material grain  
40  
41 18 size was taken into account, these reaches were found to occur at  $\omega_{vp}$  values between  
42  
43 19 empirically defined thresholds for the onset of meandering with scroll bar development  
44  
45 20 (Makaske et al., 2009; Equation 5, Figure 5) and below those required to instigate high  
46  
47 21 levels of braiding (van den Berg, 1995; Equation 3, Figure 5). They were found in  
48  
49 22 unconfined settings and were generally significantly wider than laterally stable  
50  
51 23 reaches. It is important to note that these reaches could not have been isolated on the  
52  
53 24 basis of their sinuosity alone (c.f. early classification schemes such as that of Leopold  
54  
55 25 and Wolman, 1957). A large number of laterally stable reaches had similar, and  
56  
57  
58  
59  
60

1  
2  
3 1 occasionally greater, sinuosity values than those of the laterally active sinuous-  
4  
5 2 meandering reaches identified in this study. However, as discussed above, river  
6  
7 3 energy is not the only determinant of meandering and this is evident from the lack of  
8  
9  
10 4 any clear, systematic correlation between  $\omega_{vp}$  and sinuosity. Inactive meandering  
11  
12 5 channels have been shown to exist as a product of antecedent relief (e.g. Kleinhans  
13  
14 6 et al., 2009) or as relic features formed under different process regimes (e.g.  
15  
16 7 Ferguson, 1987). This highlights the danger of classifying reaches based on simple,  
17  
18 8 individual measures of channel form. Without the inclusion of visual observations of  
19  
20 9 point bar features, longitudinal width measurements and consideration of channel form  
21  
22 10 under baseflow and active conditions as part of the classification procedure, process-  
23  
24 11 based distinction between different types of “meandering” rivers would not have been  
25  
26 12 possible.  
27  
28  
29  
30  
31  
32

33 14 Transitional (near-braided) channels exhibiting lateral and/or mid-channel bars that  
34  
35 15 become significantly wider and less sinuous with increasing flow stage were found to  
36  
37 16 occur almost exclusively under high energy conditions and above an empirically-  
38  
39 17 derived threshold for the onset of meandering with scroll and chute bar development  
40  
41 18 and moderate braiding (Kleinhans and van den Berg, 2011; Equation 4, Figure 5). The  
42  
43 19 average active width of reaches in this class was found to be significantly greater than  
44  
45 20 that of laterally stable reaches. This is consistent with channel development in  
46  
47 21 situations where local hydraulic forces significantly exceed the resistive strength of the  
48  
49 22 channel boundary. The strong contrast between the morphological configuration of  
50  
51 23 these two reach classes is shown in Figure 9. It compares the measured width of  
52  
53 24 reaches in each class with their expected width based on Equation 2. The equation  
54  
55 25 (originally derived from a data set of largely single-thread gravel bed rivers)  
56  
57  
58  
59  
60

1  
2  
3 1 systematically predicts much greater width values for laterally stable reaches than  
4  
5 2 were measured, pointing to the likely highly resistive nature of their bank materials.  
6  
7 3 However, transitional channels are predicted to be narrower than measured, indicating  
8  
9 4 a highly erodible boundary. Closer inspection of a sample of our study reaches  
10  
11 5 confirmed the presence of non-cohesive bed and bank materials. While the majority  
12  
13 6 of the transitional reaches identified through the classification procedure were found  
14  
15 7 in unconfined situations, they also occurred in confined and partially confined valleys.  
16  
17 8 This is not unusual, with many gravel bed rivers in mountain environments adopting a  
18  
19 9 “string-of-pearls” morphology, with intensely braided sections where valleys have  
20  
21 10 infilled with coarse sediment and intervening single-thread or wandering sections  
22  
23 11 where bedrock constraints restrict the valley width (Gurnell et al., 2000). This may  
24  
25 12 partially account for the high longitudinal width variation evident in this reach class.  
26  
27  
28  
29  
30  
31  
32

33 14 The remaining two reach types identified by the classification, bedrock and  
34  
35 15 cascade/step dominated channels, were both predominantly found in confined valley  
36  
37 16 situations and under very high energy conditions (primarily driven by steep valley  
38  
39 17 slopes). This natural lateral constraint acts as a major control on channel width and  
40  
41 18 sinuosity in both of these types of channels (Brierley and Fryirs, 2005) but their  
42  
43 19 distinction here is enabled by contrasting scores for particular process indicators which  
44  
45 20 are reflective of differences in sediment supply conditions. The presence of cascades  
46  
47 21 and step features, coupled with occasional lateral and/or middle channel bars and  
48  
49 22 strong longitudinal variation in width is consistent with situations in which channel  
50  
51 23 morphology is strongly influenced by sediment supply via hillslope processes and  
52  
53 24 relatively infrequent but high magnitude flood events (Montgomery and Buffington,  
54  
55 25 1997). Cascade/step dominated reaches tended to occur at significantly higher  
56  
57  
58  
59  
60

1  
2  
3 1 elevations than bedrock reaches, where the exposure of visible bedrock and the  
4  
5 2 presence of rapid features is indicative of very high transport capacity relative to the  
6  
7 3 level of sediment supply (Montgomery et al., 1996). Resistant bedrock and  
8  
9 4 consequently low bedload transport rates would account for the low to intermediate  
10  
11 5 variation in width or sinuosity with flow stage and only occasional presence of bar  
12  
13 6 features.  
14  
15  
16  
17 7

## 8 **Further applications of the use of form-based process indicators from Google** 9 **Earth in river classification**

10 The interpretability of the reach types derived in this study in relation to known controls  
11 of river morphology and behaviour suggests that form-based process indicators  
12 derived from Google Earth can provide a sound basis for river classification. While we  
13 acknowledge the importance of sources of error and limitations with the method  
14 presented, the results suggest that there are sufficiently strong links between river  
15 form and process to enable remote definition of geomorphologically-meaningful reach  
16 categories. The bottom-up nature of the method means reach types are not fixed but,  
17 instead, are determined by the data themselves. Repeating the classification on a  
18 completely different sample of rivers would not necessarily result in definition of the  
19 same five reach types and, in doing so, the approach respects the fact that river  
20 channels span a continuum without definitive, fixed thresholds between types  
21 (Ferguson, 1987; Church, 2006). It is also important to note that the resulting  
22 classification does not have to represent an “end-point”. If available, supplementary  
23 information that is not attainable from Google Earth (e.g. field measurements of grain  
24 size, depth, etc.) could be used to further categorise reaches.  
25

1  
2  
3 1 A key aim of this paper was to attempt to link channel reach types to potential  
4  
5 2 underlying physical controls that were relatively simple to define using a combination  
6  
7 3 of published data and Google Earth. However, there is a need to further validate the  
8  
9 4 findings using field surveys of boundary materials in different reach types. Likewise,  
10  
11 5 although beyond the scope of our study, the existence of an ever-expanding database  
12  
13 6 of historical imagery in Google Earth offers great potential for developing dynamic  
14  
15 7 form-based process indicators and tracking the temporal trajectories of individual  
16  
17 8 reaches as a way of characterising their geomorphological sensitivity (Fryirs, 2017).  
18  
19 9 Finally, the approach could be used to help prioritise reaches for conservation and  
20  
21 10 restoration efforts by characterising the nature and distribution in relation to physical  
22  
23 11 controls of heavily managed river reaches. They could be expected to display different  
24  
25 12 process-indicator values when compared to near-natural reaches in similar  
26  
27 13 physiographic settings. It raises the prospect that, as higher resolution data sets  
28  
29 14 become available and semi-automation is enabled via platforms such as Google Earth  
30  
31 15 Engine, reaches in disequilibrium could be quickly identified throughout catchments  
32  
33 16 and at national scales.  
34  
35  
36  
37  
38  
39  
40  
41

## 42 **CONCLUSION**

43  
44 19 In this paper, we have explored whether process-relevant dimensional and  
45  
46 20 morphological characteristics of rivers can be extracted from Google Earth via its  
47  
48 21 Google Earth Pro software application by developing a classification of transitional to  
49  
50 22 single thread river types. A geomorphologically-meaningful, empirically-based  
51  
52 23 classification of European semi-natural rivers was achieved, but it is important to  
53  
54 24 stress that its results were dependent on several factors that influenced site selection,  
55  
56 25 image selection and data extraction:  
57  
58  
59  
60

1  
2  
3 1  
4  
5 2 (i) *Careful selection of river reaches that were as free as possible of direct*  
6  
7 *geomorphological or hydrological interventions.* For testing the classification using  
8 3  
9 independent process data, we confined our search to reaches where a nearby flow  
10 4  
11 gauging station had been deemed to monitor near-natural flows or where the reach  
12 5  
13 could be seen to be unaffected by major river regulation structures;  
14 6  
15  
16  
17 7

18  
19 8 (ii) *Careful selection of images to maximise the consistency, quality and accuracy of*  
20  
21 *any measurements.* In particular, we selected images that represented baseflow  
22 9  
23 conditions, displayed good water clarity and, where there was overhanging riparian  
24 10  
25 vegetation, were captured on a date where leaf cover would not obscure the features  
26 11  
27 that are to be identified or measured;  
28 12  
29  
30  
31 13

32  
33 14 (iii) *Selection of process- and form-relevant properties that could be extracted reliably*  
34  
35 *from images.* This involved iterative development of measurement approaches and  
36 15  
37 the eventual rejection of several properties that proved too difficult to identify or to  
38 16  
39 measure consistently.  
40 17  
41  
42 18

43  
44 19 Within the constraints of focussing on the single thread to transitional planforms that  
45  
46 are characteristic of most of European river systems, five broad river types were  
47 20  
48 identified which showed expected relationships with controlling variables. This  
49 21  
50 demonstrates that if used carefully, the Google Earth information system provides a  
51 22  
52 source of identifiable and measurable process-relevant dimensional and  
53 23  
54 morphological characteristics of rivers, at least across the range of river sizes  
55 24  
56 investigated (6 m to 210 m channel width). This suggests that this freely-available  
57 25  
58  
59  
60

1  
2  
3 1 information source has enormous potential for supporting geomorphological  
4  
5 2 investigations across large and inaccessible areas and, by analysing multi-temporal  
6  
7 3 images of the same sites, investigating river changes over time.  
8  
9  
10 4

11  
12 5 As we have shown, there are limits to the types of information that can be extracted  
13  
14 6 such that field investigations cannot always be avoided. However, there is enormous  
15  
16 7 potential to undertake valuable preliminary and complementary analyses to those  
17  
18 8 conducted in the field. Understanding river form, function and dynamics and  
19  
20 9 developing and monitoring management interventions all require investigations across  
21  
22 10 a range of space and time scales. Google Earth provides an enormous free data  
23  
24 11 source that can be mined easily from the geomorphologist's desk top across many  
25  
26 12 such scales, supporting the assembly of large, reliable data sets in a very cost-  
27  
28 13 effective way.  
29  
30  
31  
32  
33  
34  
35  
36  
37  
38  
39  
40  
41  
42  
43  
44  
45  
46  
47  
48  
49  
50  
51  
52  
53  
54  
55  
56  
57  
58  
59  
60

## 1 REFERENCES

- 2 Alabyan, A.M., Chalov, R.S. (1998) Types of river channel patterns and their natural  
3 controls. *Earth Surface Processes and Landforms*, 23, 467-474.
- 4 Alber A, Piégay H. 2011. Spatial disaggregation and aggregation procedures for  
5 characterizing fluvial features at the network-scale: Application to the Rhône basin  
6 (France). *Geomorphology* 125: 343-360.
- 7 Beechie, T.J, Liermann, M., Pollock, M.M., Baker, S., Davies, J. (2006) Channel  
8 pattern and river-floodplain dynamics in forested mountain river systems.  
9 *Geomorphology*, 78, 124-141.
- 10 Bizzi, S., Demarchi, L., Grabowski, R.C., Weissteiner, C.J., van de Bund, W. 2015.  
11 The use of remote sensing to characterise hydromorphological properties of  
12 European rivers. *Aquatic Sciences*, First online, DOI: 10.1007/s00027-015-0430-7
- 13 Beldsoe, B.P., Watson, C.C. (2001) Logistic analysis of channel pattern thresholds:  
14 meandering, braiding, and incising. *Geomorphology*, 38, 281-300.
- 15 Brierley, G.J., Fryirs, K.A. (2000) River Styles, a geomorphic approach to catchment  
16 characterization: Implications for river rehabilitation in the Bega catchment, New  
17 South Wales, Australia. *Environmental Management*, 25, 661-679.
- 18 Brierley, G.J., Fryirs, K.A. (2005) *Geomorphology and River Management:  
19 Applications of the River Styles Framework*. Oxford: Blackwell Publishing, 398pp.
- 20 Buffington, J.M., Montgomery, D.R. (2013) Geomorphic classification of rivers. In  
21 Shroder, J., Wohl, E. (eds.), *Treatise on Geomorphology*. San Diego: Academic  
22 Press, vol. 9, Fluvial Geomorphology, pp. 730–767.
- 23 Church, M. (2006) Bed material transport and the morphology of alluvial river  
24 channels. *Annual Review of Earth and Planetary Sciences*, 34, 325-354.



- 1  
2  
3 1 Demarchi, L., Bizzi, S., Piegay, H. (2016) Hierarchical object-based mapping of  
4 riverscape units and in-stream mesohabitats using LiDAR and VHR imagery.  
5  
6 2  
7  
8 3 *Remote Sensing*, 8, 97.
- 9  
10 4 Demarchi, L., Bizzi, S., Piegay, H. (2017) Regional hydromorphological  
11 characterization with continuous and automated remote sensing analysis based on  
12 VHR imagery and low-resolution LiDAR data. *Earth Surface Processes and*  
13  
14 6 *Landforms*, 42, 531-551.
- 15  
16  
17 7  
18 8 Farr, T.G., Rosen, P.A., Caro, E., Crippen, R., Duren, R., Hensley, S., Kobrick, M.,  
19 Paller, M., Rodriguez, E., Roth, L., Seal, D., Shaffer, S., Shimada, J., Umland, J.,  
20  
21 9  
22 10 Werner, M., Oskin, M., Burbank, D., Alsdorf, D. (2007) The Shuttle Radar  
23 Topography Mission. *Reviews of Geophysics*, 45, RG2004.
- 24  
25  
26 11  
27 12 Ferguson, R.I. (1984) The threshold between meandering and braiding. *Channels and*  
28  
29 13 *Channel Control Structures*, 6, 15–29.
- 30  
31  
32 14 Ferguson, R.I. (1987) Hydraulic and sedimentary controls of channel patterns. in K.S.  
33 Richards (ed.), *River Channels: Environment and Processes*. Oxford: Blackwell, pp.  
34  
35 15  
36 16 129–158.
- 37  
38  
39 17 Frissell, C.A., Liss, W.J., Warren, C.E., Hurley, M.D. (1986) A hierarchical framework  
40 for stream habitat classification: Viewing streams in a watershed context.  
41  
42 18  
43 19 *Environmental Management*, 10, 199-214.
- 44  
45  
46 20 Fryirs, K. (2017) River sensitivity: a lost foundation concept in fluvial geomorphology.  
47  
48 21 *Earth Surface Processes and Landforms*, 42, 55-70.
- 49  
50  
51 22 Giri, C., Ochieng, E., Tieszen, L.L., Zhu, Z., Singh, A., Loveland, T., Masek, J., Duke,  
52  
53 23 N. (2010) Status and distribution of mangrove forests of the world using earth  
54 observation satellite data. *Global Ecology and Biogeography*, 20, 154-159.  
55  
56  
57  
58  
59  
60

- 1  
2  
3 1 Gorelick, N., Hancher, M., Dixon, M., Ilyushchenko, S., Thau, D., Moore, R. (2017)  
4  
5 2 Google Earth Engine: Planetary-scale geospatial analysis for everyone. *Remote*  
6  
7 3 *Sensing of Environment*, 202, 18-27.  
8  
9  
10 4 Gurnell, A.M., Petts, G.E., Harris, N., Ward, J.V., Tockner, K., Edwards, P.J.,  
11  
12 5 Kollmann, J. (2000) Large wood retention in river channels: the case of the Fiume  
13  
14 6 Tagliamento, Italy. *Earth Surface Processes and Landforms*, 2000, 25, 255-275.  
15  
16  
17 7 Gurnell, A.M. Rinaldi, M., Belletti, B., Bizzi, S., Blameur, B., Braca, G., Buijse, T.,  
18  
19 8 Bussentini, M., Camenen, B., Comiti, F., Demarchi, L., Garcia de Jalon, D.,  
20  
21 9 Gonzalez, del Tanago, M, Grabowski, R., Gunn, I., Habersack, H., Hendriks, D.,  
22  
23 10 Henshaw, A.J., Klosch, M., Lastoria, B., Latapie, A., Marcinkowski, P., Martinez-  
24  
25 11 Fernandez, V., Mosselmann, E., Mountford, J.O., Nardi, L., Okruszko, T., O'Hare,  
26  
27 12 M.T., Palma, M., Percopo, C., Surian, N., van de Bund, W., Weissteiner, C., Ziliani,  
28  
29 13 L. (2016) A multi-scale hierarchical framework for developing understanding of river  
30  
31 14 behaviour to support river management. *Aquatic Sciences*, 78, 1-16.  
32  
33  
34 15 Hey, R.D., Thorne, C.R. (1986) Stable channels with mobile gravel beds. *Journal of*  
35  
36 16 *Hydraulic Engineering*, 112, 671-689.  
37  
38  
39 17 Holloway, J.V., Rillig, M.C., Gurnell, A.M. (2017) Underground riparian wood: Buried  
40  
41 18 stem and coarse root structures of Black Poplar (*Populus nigra* L.). *Geomorphology*,  
42  
43 19 279, 188-198.  
44  
45  
46 20 Huang, H.Q., Chang, H.H., Nanson, G.C. (2004) Minimum energy as the general form  
47  
48 21 of critical flow and maximum flow efficiency and for explaining variation in channel  
49  
50 22 pattern. *Water Resources Research*, 40, W04502.  
51  
52  
53 23 Isikdogan, F., Bovik, A., Passalacqua, P. (2017) RivaMap: An automated river analysis  
54  
55 24 and mapping engine. *Remote Sensing of Environment*, 202, 88-97.  
56  
57  
58  
59  
60

- 1  
2  
3 1 Janes, V.J.J., Nicholas, A.P., Collins, A.L., Quine, T.A. (2017) Analysis of fundamental  
4  
5 2 physical factors influencing channel bank erosion: results for contrasting  
6  
7 3 catchments in England and Wales. *Environmental Earth Sciences*, 76, 307.  
8  
9  
10 4 Kasprak, A., Hough-Snee, N., Beechie, T., Bouwes, N., Brierley, G., Camp, R., Fryirs,  
11  
12 5 K., Imaki, H., Jensen, M., O'Brien, G., Rosgen, D., Wheaton, J. (2016) The blurred  
13  
14 6 line between form and process: a comparison of stream channel classification  
15  
16 7 frameworks. *PLoS ONE*, 11, e0150293.  
17  
18  
19 8 Kleinhans, M.G., Schuurman, F., Bakx, W, Markies, H. (2009) Meandering channel  
20  
21 9 dynamics in highly cohesive sediment on an intertidal mud flat in the Westerschelde  
22  
23 10 estuary, the Netherlands. *Geomorphology*, 105, 261-279.  
24  
25  
26 11 Kleinhans, M.G., van den Berg, J.H. (2011) River channel and bar patterns explained  
27  
28 12 and predicted by an empirical and a physics-based method. *Earth Surface*  
29  
30 13 *Processes and Landforms*, 36, 721-738.  
31  
32  
33 14 Knighton, A.D. (1998) *Fluvial forms and processes. A New Perspective*. London:  
34  
35 15 Edward Arnold.  
36  
37  
38 16 Kondolf, G.M., Piegay, H., Schmitt, L., Montgomery, D.R. (2016) Geomorphic  
39  
40 17 classification of rivers and streams. In G.M. Kondolf, H. Piegay (eds), *Tools in*  
41  
42 18 *Fluvial Geomorphology*. Chichester: John Wiley & Sons Ltd, pp. 133-158.  
43  
44  
45 19 Large, A.R.G., Gilvear, D.J. (2015) Using Google Earth, a virtual-globe imaging  
46  
47 20 platform, for ecosystem services-based river assessment. *River Research and*  
48  
49 21 *Applications*, 31, 406-421.  
50  
51  
52 22 Lave, R. (2009) The controversy over Natural Channel Design: substantive  
53  
54 23 explanations and potential avenues for resolution. *Journal of the American Water*  
55  
56 24 *Resources Association*, 45, 1519-1532.  
57  
58  
59  
60

- 1  
2  
3 1 Leopold, L.B, Wolman, G.M. (1957) *River Channel Patterns: Braided, Meandering and*  
4  
5 2 *Straight*. U.S Geological Survey Professional Paper 282-B, pp. 39–85.  
6  
7  
8 3 Makaske B., Smith, D., Berendsen, H., de Boer, A., van Nielen-Kiezebrink, M.,  
9  
10 4 Locking, T. (2009) Hydraulic and sedimentary processes causing anastomosing  
11  
12 5 morphology of the upper Columbia River, British Columbia, Canada.  
13  
14 6 *Geomorphology*, 111, 194-205.  
15  
16  
17 7 Marcus, A., Fonstad, M. 2010. Remote sensing of rivers: the emergence of a  
18  
19 8 subdiscipline in the river sciences. *Earth Surface Processes and Landforms*  
20  
21 9 35:1867–1872.  
22  
23  
24 10 Monegaglia, F., Zolezzi, G., Güneralp, I., Henshaw, A.J., Tubino, M. (2018) Automated  
25  
26 11 extraction of meandering river morphodynamics from multitemporal remotely  
27  
28 12 sensed data. *Environmental Modelling and Software*, 105, 171-186.  
29  
30  
31 13 Montgomery, D.R., Buffington, J.M. (1997) Channel-reach morphology in mountain  
32  
33 14 drainage basins. *GSA Bulletin*, 109, 596-611.  
34  
35  
36 15 Montgomery, D.R., Abbe, T.B., Buffington, J.M., Peterson, N.P., Schmidt, K.M., Stock,  
37  
38 16 J.D. (1996) Distribution of bedrock and alluvial channels in forested mountain  
39  
40 17 drainage basins. *Nature*, 381, 587-589.  
41  
42  
43 18 Naiman, R.J. (1998) Biotic stream classification. In R.J. Naiman, R.E. Bilby (eds),  
44  
45 19 *River ecology and management: lessons from the Pacific Coastal ecoregion*. New  
46  
47 20 York: Springer-Verlag.  
48  
49  
50 21 Patel, N.N., Angiuli, E., Gamba, P., Gaughan, A., Lisini, G., Stevens, F.R., Tatem, A.J.,  
51  
52 22 Trianni, G. (2015) Multitemporal settlement and population mapping from Landsat  
53  
54 23 using Google Earth Engine. *International Journal of Applied Earth Observation and*  
55  
56 24 *Geoinformation*, 35, 199-208.  
57  
58  
59  
60

- 1  
2  
3 1 Pekel, J-F., Cottam, A., Gorelick, N., Belward, A.S. (2016) High-resolution mapping of  
4  
5 2 global surface water and its long-term changes. *Nature*, 540, 418-422.  
6  
7  
8 3 Rosgen, D.L. (1994) A classification of natural rivers. *Catena*, 22, 169-199.  
9  
10 4 Schmitt R, Bizzi S, Castelletti A. 2014. Characterizing fluvial systems at basin scale  
11  
12 5 by fuzzy signatures of hydromorphological drivers in data scarce environments.  
13  
14 6 *Geomorphology*. doi: 10.1016/j.geomorph.2014.02.024  
15  
16  
17 7 Schumm, S.A. (1977) *The Fluvial System*. New York: Wiley, pp. 338.  
18  
19 8 Simon, A., Doyle, M., Kondolf, M., Shields Jr, F.D., Rhoads, B., McPhillips, M. (2007)  
20  
21 9 Critical evaluation of how the Rosgen Classification and associated “Natural  
22  
23 10 Channel Design” methods fail to integrate and quantify fluvial processes and  
24  
25 11 channel response. *Journal of the American Water Resources Association*, 43,  
26  
27 12 1117-1131.  
28  
29  
30 13 Stahl, K., Hisdal, J., Hannaford, J., Tallaksen, L., Van Lanen, H., Sauquet, E., Demuth,  
31  
32 14 S., Fendekova, M., Jordar, J. (2010) Streamflow trends in Europe: evidence from a  
33  
34 15 dataset of near-natural catchments. *Hydrology and Earth System Sciences*, 14,  
35  
36 16 2367-2382.  
37  
38  
39 17 Tadaki, M., Brierley, G., Cullum, C. (2014) River classification: theory, practice,  
40  
41 18 politics. *WIREs Water*, 1, 349-367.  
42  
43  
44 19 Tockner, K., Ward, J.V., Arscott, D.B., Edwards, P.J., Kollmann, J., Gurnell, A.M.,  
45  
46 20 Petts, G.E., Maiolini, B. (2003) The Tagliamento River: a model ecosystem of  
47  
48 21 European importance. *Aquatic Sciences*, 65, 239-253.  
49  
50  
51 22 Tockner, K., Uehlinger, U., Robinson, C.T. (2009) *Rivers of Europe*. London: Elsevier,  
52  
53 23 pp. 728.  
54  
55  
56  
57  
58  
59  
60

- 1  
2  
3 1 Tooth, S., McCarthy, T.S. (2004) Anabranching in mixed bedrock-alluvial rivers: the  
4  
5 2 example of the Orange River above Augrabies Falls, Northern Cape Province,  
6  
7 3 South Africa. *Geomorphology*, 57, 235-262.  
8  
9  
10 4 van den Berg, J.H. (1995) Prediction of alluvial channel pattern of perennial rivers.  
11  
12 5 *Geomorphology*, 12, 259-279.  
13  
14 6 Wheaton, JM, Fryirs, KA, Brierley, G, Bangen, SG, Bouwes, N, O'Brien, G. (2015)  
15  
16 7 Geomorphic mapping and taxonomy of fluvial landforms. *Geomorphology*, 248,  
17  
18 8 273-295.  
19  
20  
21  
22  
23

## 24 10 **ACKNOWLEDGEMENTS**

25  
26 11 The research for this paper was conducted within the SMART Joint Doctoral  
27  
28 12 programme (Science for the MAnagement of Rivers and their Tidal systems) funded  
29  
30 13 with the support of the Erasmus Mundus programme of the European Union. The  
31  
32 14 authors would like to thank the National River Flow Archive (United Kingdom),  
33  
34 15 Ministere de L'ecologie, du developpement durable et de l'energie (France), and  
35  
36 16 Centro de Estudios Hidrograficos de CEDEX (Spain) for the provision of river flow  
37  
38 17 records. Lastly and most importantly, the authors thank Google Earth and the many  
39  
40 18 contributing companies who have provided the aerial imagery across Europe that has  
41  
42 19 made this research possible, including Image Landsat, Infoterra Ltd and Bluesky,  
43  
44 20 Getmapping plc, Digital Globe, IGN France, GeoBasis-DE/BKG, Cnes/Spot Image,  
45  
46 21 Geoimage Austria, Eurosense/Geodis Slovakia, CNES/Austrium, MGGP Aero,  
47  
48 22 Lantmaateriet/Metria, and Geodis Brno. Alan Kasprak and an anonymous reviewer  
49  
50 23 provided valuable comments which helped strengthen this paper.  
51  
52  
53  
54  
55  
56  
57  
58  
59  
60

## 1 **Figure Captions**

2 *Figure 1: Locations of the 68 rivers from which data for 194 reaches were extracted.*

3  
4 *Figure 2: Dendrogram showing truncation (dashed line) of study reaches into five*  
5 *classes by AHC using Ward's algorithm and an entropy-based solution.*

6  
7 *Figure 3: Scatter plots showing the distribution of the 194 reaches and their class*  
8 *membership with respect to PCs 1 to 4.*

9  
10 *Figure 4: Frequency of fully (C), partly (P) and unconfined (U) reaches in each river*  
11 *class.*

12  
13 *Figure 5: Distribution of reaches in each river class in relation to elevation.*

14  
15 *Figure 6: Distribution of reaches in each river class in relation to the two year return*  
16 *period flood discharge,  $Q_2$ , and valley slope,  $S_v$ .*

17  
18 *Figure 7: Distribution of reaches of different classes in relation to bed material grain*  
19 *size and potential specific stream power. Lines represent empirically-derived*  
20 *discriminators of channels types from van den Berg (1995), Kleinhans and van den*  
21 *Berg (2011) and Maskaske et al. (2009), respectively. Bed material grain size*  
22 *estimates were not available for any rivers in classes D and E.*

23

1  
2  
3 1 *Figure 8: Relationships between potential specific stream power and a) active*  
4  
5 2 *channel width; and b) active channel sinuosity.*  
6  
7

8  
9 3

10  
11 4 *Figure 9: Comparison between measured active width and predicted width according*  
12  
13 5 *to Equation 2 (from Kleinhans and van den Berg, 2011).*  
14  
15  
16  
17  
18  
19  
20  
21  
22  
23  
24  
25  
26  
27  
28  
29  
30  
31  
32  
33  
34  
35  
36  
37  
38  
39  
40  
41  
42  
43  
44  
45  
46  
47  
48  
49  
50  
51  
52  
53  
54  
55  
56  
57  
58  
59  
60

For Peer Review



1 **Tables**

2

| Dimension (units)  | Description   | Relationship to fluvial processes   |
|--|---|---|
| <b>Extracted from Google Earth</b>                             |   |   |
| Upstream elevation (m)   | Elevation of the lower bank top at the upstream end of the reach.   |   |
| Downstream elevation (m)                                       | Elevation of the lower bank top at the downstream end of the reach.   |   |
| Valley length (m)  | Sum of straight line lengths between channel bend inflection points.  |   |
| Active reach length (m)  | Mid-line length of channel whose edges are defined by continuous vegetation cover (unvegetated bars are part of channel width).   |   |
| Baseflow reach length (m)                                      | Mid-line length of inundated channel at baseflow.   |   |
| Active channel width (m)                                       | Width of the channel within the reach whose edges are defined by continuous vegetation cover (10 measurements taken at equally spaced intervals along the active channel mid-line). |   |
| Baseflow channel width (m)                                     | Water width (excluding exposed bars) at baseflow (2 measurements taken at locations where water width is at a minimum and maximum within the reach).                                |   |
| <b>Derived variables</b>                                       |   |   |
| Active channel sinuosity                                       | Active reach length / Valley length   |   |
| Baseflow channel sinuosity                                     | Baseflow reach length / Valley length   |   |
| Active slope (m/m)   | (Upstream elevation – Downstream elevation) / Active reach length   |   |
| Baseflow slope (m/m)   | (Upstream elevation – Downstream elevation) / Baseflow reach length   |   |
| Valley slope (m/m)   | (Upstream elevation – Downstream elevation) / Valley length   |   |
| <b>Derived variables used in Principal Components Analysis</b> |   |   |
| Active channel sinuosity                                       | See above   | Capacity for lateral adjustment in meandering rivers (Janes et al., 2017)   |
| Baseflow: Active channel sinuosity                             | (Baseflow reach length / Valley length) / (Active reach length / Valley length)   | Indicative of bank erodibility relative to stream power and/or bed material supply rate (Carson, 1984; Ferguson, 1987). |
| Active: Baseflow channel width                                 | (Median active channel width) / (Median baseflow channel width)   | Proxy for width:depth ratio, indicates bank resistance relative to stream power (Eaton                                  |

|    |                          |  |                           |
|----|--------------------------|--|---------------------------|
| 1  |                          |  |                           |
| 2  |                          |  |                           |
| 3  |                          |  | and Millar, 2004);        |
| 4  |                          |  | response to changes in    |
| 5  |                          |  | sediment load             |
| 6  |                          |  | (Schumm, 1977); active    |
| 7  |                          |  | (transporting) width      |
| 8  |                          |  | (Garcia Lugo et al.,      |
| 9  |                          |  | 2015)                     |
| 10 | Coefficient of variation | (Standard deviation of active channel width) / | Strong longitudinal       |
| 11 | of active channel width  | (Mean active channel width)                    | variation in channel      |
| 12 |                          |  | width associated with     |
| 13 |                          |  | increased                 |
| 14 |                          |  | morphological activity in |
| 15 |                          |  | meandering rivers that    |
| 16 |                          |  | reflects variability in   |
| 17 |                          |  | flow and sediment         |
| 18 |                          |  | transport and bank        |
| 19 |                          |  | material properties       |
| 20 |                          |  | (Lagasse et al. 2004;     |
| 21 |                          |  | Zolezzi et al., 2012)     |

1 *Table 1: Channel dimensions extracted from Google Earth images and dimension*  
 2 *indices used in Principal Components Analysis.*

3

| Feature                | Description   | Relationship to fluvial processes  |
|------------------------|---|--|
| Active lateral bar     | Depositional feature attached to the river bank but not on the inside of a river bend with no significant vegetation cover and extending into the channel for at least 20% of the bankfull width. | Correlation between increasing frequency of bars and sediment supply rate (Brierley and Fryirs, 2005)  |
| Active point bar       | Depositional feature attached to the river bank on the inside of a river bend with no significant vegetation cover and extending into the channel for at least 20% of the bankfull width          | Correlation between increasing frequency of bars and sediment supply rate (Brierley and Fryirs, 2005)  |
| Active mid-channel bar | Mid-channel depositional feature with no significant vegetation cover that is not attached to the banks at normal flow and occupies a minimum of 20 % channel width                               | Presence indicates high rates of sediment supply and morphological activity (Brierley and Fryirs, 2005)  |
| Channel cutoff         | Recent or historic channel cutoff (can be wet or dry but is clearly visible on floodplain)  | Presence indicates high rates of recent or historical morphological activity (Kleinhans and van den Berg, 2011)  |
| Bedrock                | Area of exposed bedrock forming a semi-continuous surface close to or exposed through the water surface.  | Indicative of high energy, supply-limited transport conditions (Brierley and Fryirs, 2005)   |
| Cascade                | Area of highly disturbed water tumbling over and around disorganised boulders   | Presence indicates supply-limited transport regime and strong influence of non-fluvial (e.g. hillslope, glacial, etc.) processes (Montgomery and Buffington, 1997) |
| Step                   | Flow falls near vertically over single channel-spanning line of large clasts causing disturbance to water surface.  | Presence indicates supply-limited transport regime but greater influence of fluvial processes than cascade-dominated reaches (Montgomery and Buffington, 1997)     |
| Rapids                 | Sequences of partially or fully channel-spanning, organised ribs with fewer exposed boulders than cascades but greater areal proportion of disturbed water surface than riffles                   | Presence indicative of transport-limited conditions but greater transport capacity than riffle-dominated reaches (Brierley and Fryirs, 2005)                       |
| Riffle                 | Area of disturbed water surface with negligible bed material exposure   | Presence indicative of transport-limited conditions (Brierley and Fryirs, 2005)  |

1 *Table 2: Definitions of features identified and counted from Google Earth images.*

2

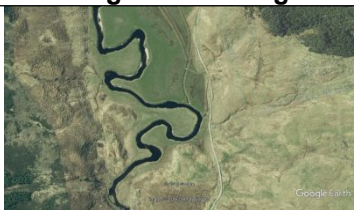




|  | PC1          | PC2          | PC3          | PC4           |
|--|--------------|--------------|--------------|---------------|
| <b>BEFORE ROTATION</b>                           |              |              |              |               |
| Eigenvalue                                       | 4.209        | 2.709        | 1.524        | 1.157         |
| Variability (%)                                  | 32.380       | 20.840       | 11.723       | 8.898         |
| Cumulative %                                     | 32.380       | 53.221       | 64.944       | 73.841        |
| <b>AFTER ROTATION</b>                            |              |              |              |               |
| Variability (%)                                  | 31.199       | 15.638       | 11.491       | 15.513        |
| Cumulative %                                     | 31.199       | 46.838       | 58.328       | 73.841        |
| <b>LOADINGS</b>                                  |              |              |              |               |
| Active channel sinuosity                         | -0.596       | 0.589        | -0.099       | -0.201        |
| Baseflow:Active channel sinuosity                | <b>0.816</b> | 0.392        | -0.021       | 0.043         |
| Active:Baseflow channel width                    | <b>0.827</b> | -0.112       | 0.145        | 0.169         |
| Coefficient of variation of active channel width | <u>0.692</u> | -0.004       | -0.215       | 0.199         |
| Active lateral bars                              | <b>0.910</b> | -0.033       | 0.140        | -0.053        |
| Active mid-channel bars                          | <b>0.800</b> | -0.054       | 0.110        | -0.125        |
| Active point bars                                | 0.098        | <b>0.853</b> | 0.048        | -0.187        |
| Channel cutoffs                                  | 0.006        | <b>0.736</b> | -0.241       | -0.138        |
| Bedrock  | -0.069       | -0.017       | <b>0.859</b> | 0.259         |
| Cascades   | 0.167        | -0.284       | 0.071        | <b>0.857</b>  |
| Steps  | 0.211        | -0.314       | -0.085       | <b>0.767</b>  |
| Rapids   | 0.249        | -0.224       | <b>0.746</b> | -0.260        |
| Riffles  | 0.504        | -0.127       | -0.138       | <u>-0.614</u> |

1 *Table 3: Eigenvalues, percentage variability explained (before and after a varimax*  
2 *rotation), and variable loadings on the first four PCs of a Principal Components*  
3 *Analysis of channel dimension and physical feature variables. (Note that loadings >*  
4 *0.7 are emboldened and loadings > 0.6 and <0.7 are in italics and underlined).*




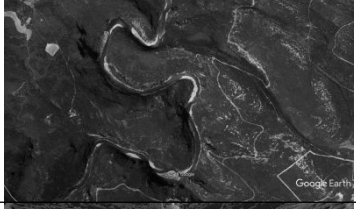

| Variable | K     | DF | p       | Significant differences between classes | Bonferroni corrected significance level |
|----------|-------|----|---------|---|---|
| PC1      | 123.8 | 4  | <0.0001 | C, E > A, D    B > A                    | 0.005                                   |
| PC2      | 91.1  | 4  | <0.0001 | B > A, C, D, E    A > C, E              | 0.005                                   |
| PC3      | 75.3  | 4  | <0.0001 | D > A, B, C, E    B, C, D > E           | 0.005                                   |
| PC4      | 112.3 | 4  | <0.0001 | E > A, B, C    A, B, D > C              | 0.005                                   |

1 *Table 4: Results of Kruskal-Wallis tests (followed by multiple pairwise comparisons,*  
2 *based on Dunn's procedure with Bonferroni correction), applied to PC scores on each*  
3 *of the 5 clusters identified using agglomerative hierarchical clustering.*

For Peer Review

| Class    | PC1 | PC2 | PC3 | PC4 | Description                 | Example                               | Google Earth image  |
|----------|-----|-----|-----|-----|-----------------------------|---------------------------------------|---|
| <b>A</b> | -   |     |     |     | Laterally stable            | Abhainn an t-Strath Chuileannach (UK) |    |
| <b>B</b> | +   | +   |     |     | Active sinuous-meandering   | Allier (France)                       |    |
| <b>C</b> | +   | -   |     | -   | Transitional (near-braided) | Feshie (UK)                           |    |
| <b>D</b> |     |     | +   | +   | Bedrock                     | Ardèche (France)                      |   |
| <b>E</b> | +   | -   | -   | +   | Cascade/step dominated      | Bregenzer Ach (Austria)               |  |

1 *Table 5: Summary of the range (+ = positive, - = negative, blank = intermediate) of*  
2 *significantly different PC scores for reaches in each class in relation to each PC, and*  
3 *a brief description of each class based on interpretation of the environmental gradients*  
4 *described by each PC. (All images obtained from Google Earth. Additional copyright*  
5 *attributions: Allier - Image © 2018 CNES/Airbus, Image © 2018 DigitalGlobe; Feshie*  
6 *– Image © Getmapping plc; Abhainn an t-Strath Chuileannach – Image © 2018*  
7 *Getmapping plc; Ardèche – Image © 2018 Google; Bregenzer Ach – Image © 2009*  
8 *Geobasis-DE/BKG, Image © 2018 DigitalGlobe, Image © 2018 Google).*

| Class    | PC1 | PC2 | PC3 | PC4 | Description                 | Example                               | Google Earth image  |
|----------|-----|-----|-----|-----|-----------------------------|---------------------------------------|---|
| <b>A</b> | -   |     |     |     | Laterally stable            | Abhainn an t-Strath Chuileannach (UK) |    |
| <b>B</b> | +   | +   |     |     | Active sinuous-meandering   | Allier (France)                       |    |
| <b>C</b> | +   | -   |     | -   | Transitional (near-braided) | Feshie (UK)                           |    |
| <b>D</b> |     |     | +   | +   | Bedrock                     | Ardèche (France)                      |   |
| <b>E</b> | +   | -   | -   | +   | Cascade/step dominated      | Bregenzer Ach (Austria)               |  |

1 **Table 5: GREYSCALE VERSION FOR PRINT VERSION** Summary of the range (+ =  
2 positive, - = negative, blank = intermediate) of significantly different PC scores for  
3 reaches in each class in relation to each PC, and a brief description of each class  
4 based on interpretation of the environmental gradients described by each PC. (All  
5 images obtained from Google Earth. Additional copyright attributions: Allier - Image ©  
6 2018 CNES/Airbus, Image © 2018 DigitalGlobe; Feshie – Image © Getmapping plc;  
7 Abhainn an t-Strath Chuileannach – Image © 2018 Getmapping plc; Ardèche – Image  
8 © 2018 Google; Bregenzer Ach – Image © 2009 Geobasis-DE/BKG, Image © 2018  
9 DigitalGlobe, Image © 2018 Google).

1  
2  
3  
4  
5  
6  
7  
8  
9  
10  
11  
12  
13  
14  
15  
16  
17  
18  
19  
20  
21  
22  
23  
24  
25  
26  
27  
28  
29  
30  
31  
32  
33  
34  
35  
36  
37  
38  
39  
40  
41  
42  
43  
44  
45  
46  
47  
48  
49  
50  
51  
52  
53  
54  
55  
56  
57  
58  
59  
60

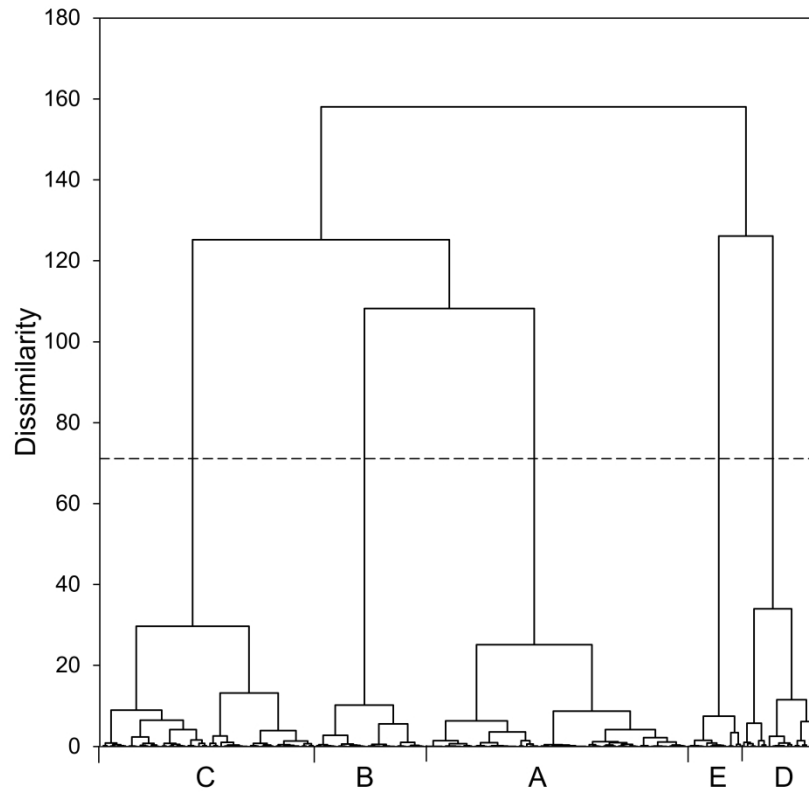


Figure 2: Dendrogram showing truncation (dashed line) of study reaches into five classes by AHC using Ward's algorithm and an entropy-based solution.

504x464mm (150 x 150 DPI)



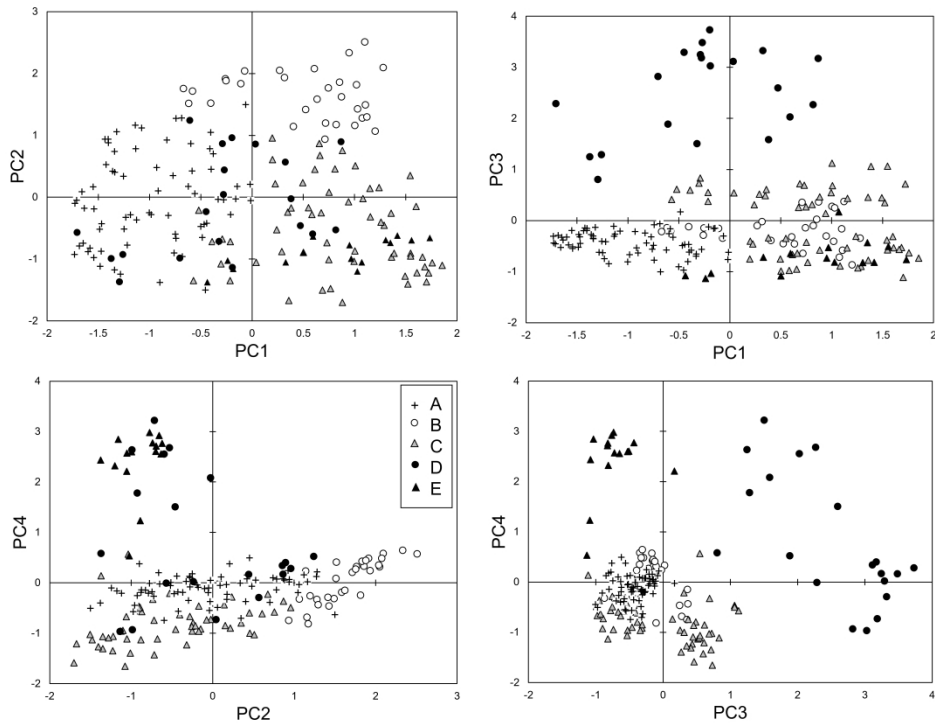


Figure 3: Scatter plots showing the distribution of the 194 reaches and their class membership with respect to PCs 1 to 4.

799x606mm (150 x 150 DPI)

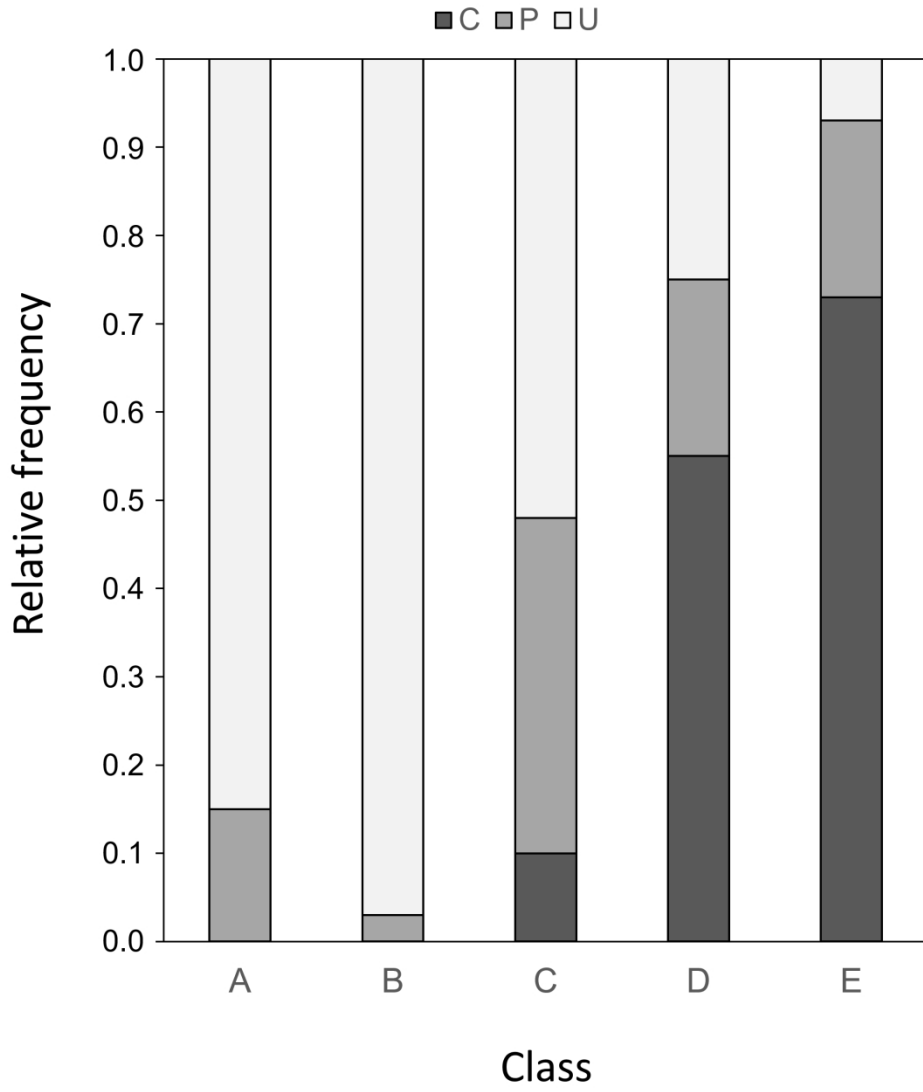


Figure 4: Frequency of fully (C), partly (P) and unconfined (U) reaches in each river class.

417x501mm (150 x 150 DPI)

1  
2  
3  
4  
5  
6  
7  
8  
9  
10  
11  
12  
13  
14  
15  
16  
17  
18  
19  
20  
21  
22  
23  
24  
25  
26  
27  
28  
29  
30  
31  
32  
33  
34  
35  
36  
37  
38  
39  
40  
41  
42  
43  
44  
45  
46  
47  
48  
49  
50  
51  
52  
53  
54  
55  
56  
57  
58  
59  
60

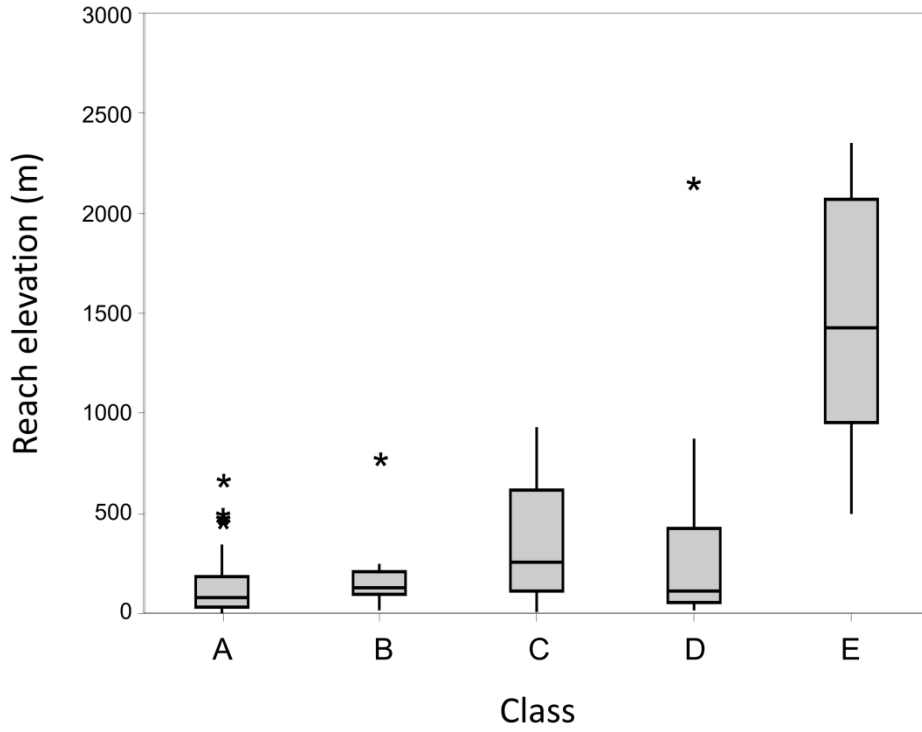


Figure 5: Distribution of reaches in each river class in relation to elevation.

561x479mm (150 x 150 DPI)

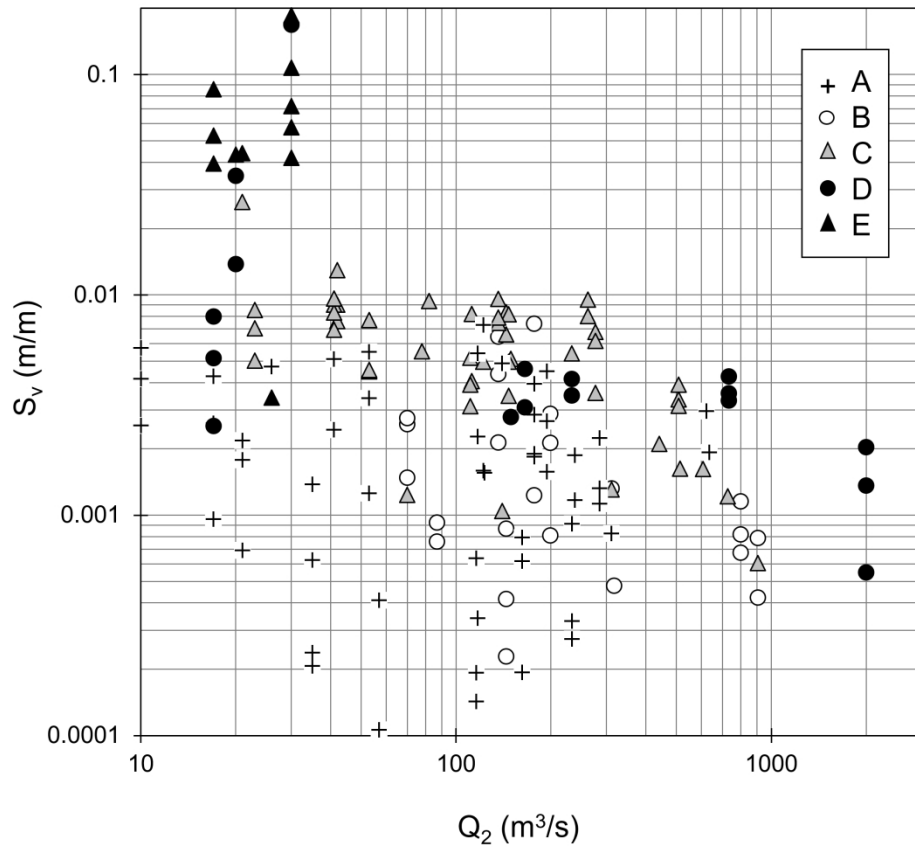


Figure 6: Distribution of reaches in each river class in relation to the two year return period flood discharge,  $Q_2$ , and valley slope,  $S_v$ .

472x460mm (150 x 150 DPI)

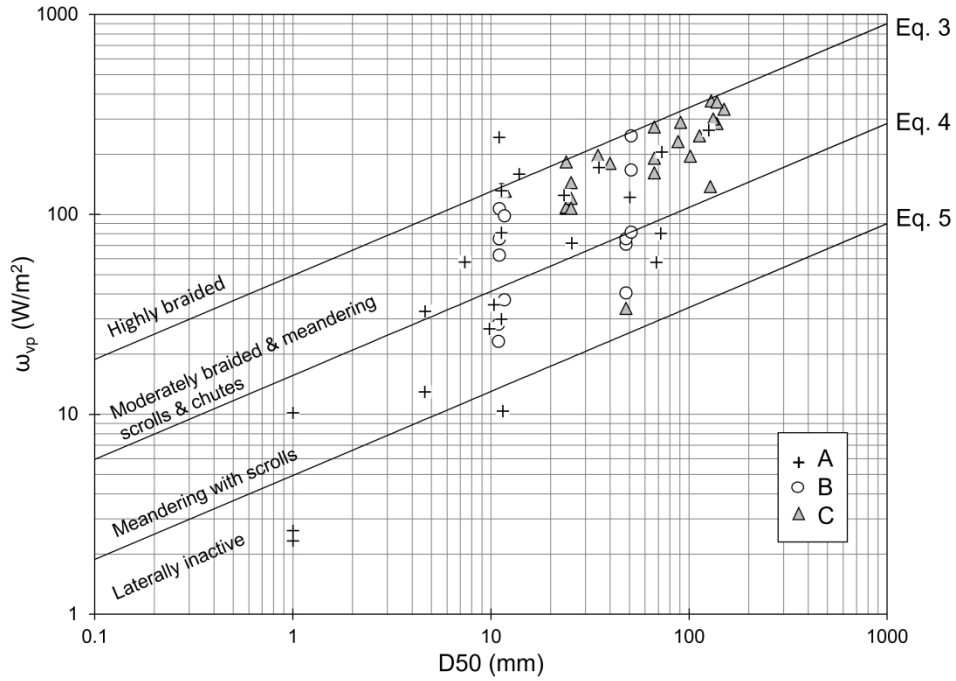


Figure 7: Distribution of reaches of different classes in relation to bed material grain size and potential specific stream power. Lines represent empirically-derived discriminators of channels types from van den Berg (1995), Kleinhans and van den Berg (2011) and Maskaske et al. (2009), respectively. Bed material grain size estimates were not available for any rivers in classes D and E.

590x417mm (150 x 150 DPI)

1  
2  
3  
4  
5  
6  
7  
8  
9  
10  
11  
12  
13  
14  
15  
16  
17  
18  
19  
20  
21  
22  
23  
24  
25  
26  
27  
28  
29  
30  
31  
32  
33  
34  
35  
36  
37  
38  
39  
40  
41  
42  
43  
44  
45  
46  
47  
48  
49  
50  
51  
52  
53  
54  
55  
56  
57  
58  
59  
60

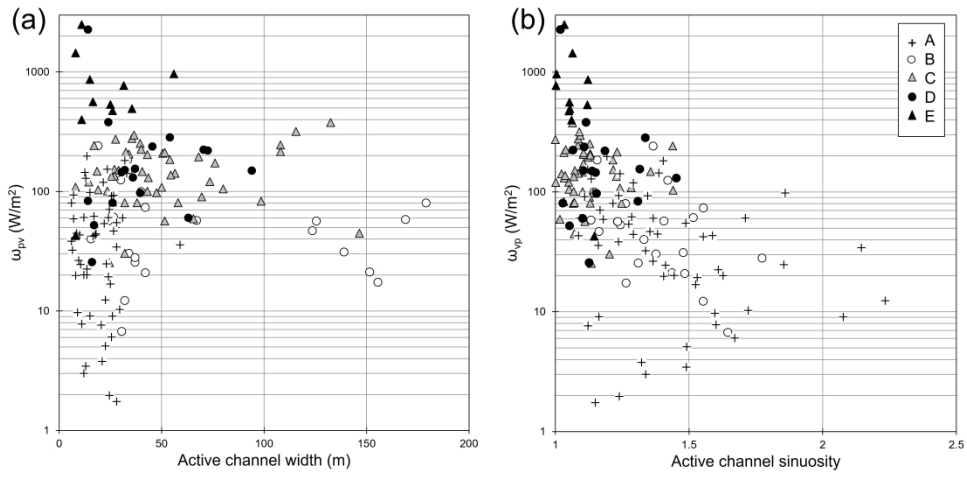


Figure 8: Relationships between potential specific stream power and a) active channel width; and b) active channel sinuosity.

889x442mm (150 x 150 DPI)

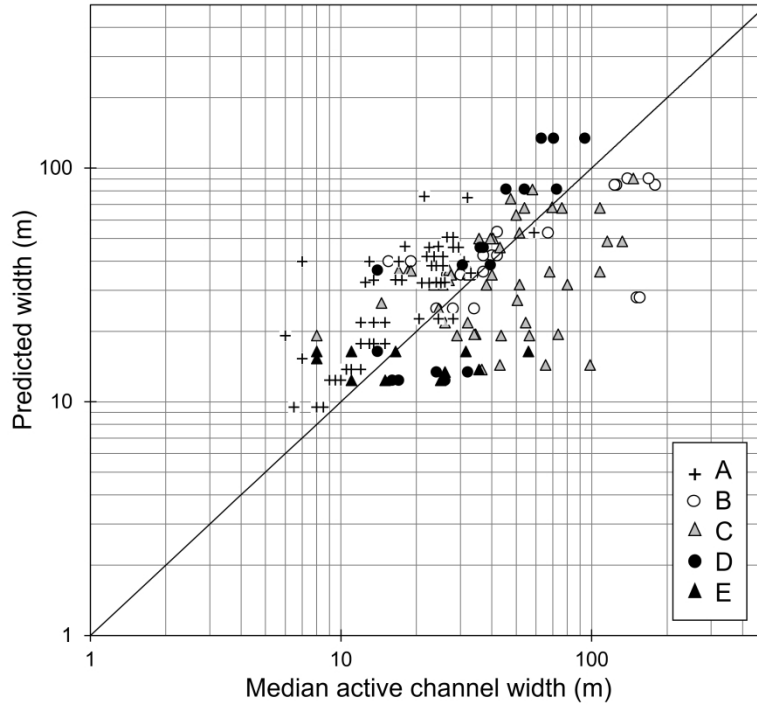


Figure 9: Comparison between measured active width and predicted width according to Equation 2 (from Kleinhans and van den Berg, 2011).

552x449mm (150 x 150 DPI)